REVISED

Limits of Wave Runup and Corresponding Beach-Profile Change from Large-Scale Laboratory Data

TIFFANY M. ROBERTS[†], PING WANG[†], and NICHOLAS C. KRAUS[‡]

[†]: Department of Geology, University of South Florida, 4202 E. Fowler Ave., Tampa, FL 33620, USA. (E-mail: tmrobert@cas.usf.edu)

[‡]: U.S. Army Engineer Research and Development Center, Coastal and Hydraulics Laboratory, 3909 Halls Ferry Road, Vicksburg, MS 39180-6199, USA.

Report Documentation Page

Form Approved
OMB No. 0704-0188

1. REPORT DATE	2. REPORT TYPE	3. DATES COVERED
2009		**00-00-2009 to 00-00-2009**

4. TITLE AND SUBTITLE	5a. CONTRACT NUMBER
Limits of Wave Runup and Corresponding Beach-Profile Change from Large-Scale Laboratory Data	5b. GRANT NUMBER
	5c. PROGRAM ELEMENT NUMBER
6. AUTHOR(S)	5d. PROJECT NUMBER
	5e. TASK NUMBER
	5f. WORK UNIT NUMBER
7. PERFORMING ORGANIZATION NAME(S) AND ADDRESS(ES) **Department of Geology,University of South Florida,4202 E. Fowler Ave,Tampa,FL,33620**	8. PERFORMING ORGANIZATION REPORT NUMBER
9. SPONSORING/MONITORING AGENCY NAME(S) AND ADDRESS(ES)	10. SPONSOR/MONITOR'S ACRONYM(S)
	11. SPONSOR/MONITOR'S REPORT NUMBER(S)

12. DISTRIBUTION/AVAILABILITY STATEMENT
Approved for public release; distribution unlimited

13. SUPPLEMENTARY NOTES

14. ABSTRACT

15. SUBJECT TERMS

16. SECURITY CLASSIFICATION OF:			17. LIMITATION OF ABSTRACT	18. NUMBER OF PAGES	19a. NAME OF RESPONSIBLE PERSON
a. REPORT **unclassified**	b. ABSTRACT **unclassified**	c. THIS PAGE **unclassified**	**Same as Report (SAR)**	**57**	

18
19 **ABSTRACT**

20 The dataset from the SUPERTANK laboratory experiment was analyzed to
21 examine wave runup and the corresponding upper limit of beach-profile change. Thirty
22 SUPERTANK runs were investigated that included both erosional and accretionary wave
23 conditions with random and monochromatic waves. The upper limit of beach change U_L
24 was found to approximately equal the vertical excursion of total wave runup, R_{tw}. An
25 exception was runs where beach or dune scarps were produced, which substantially limit
26 the uprush of swash motion to produce a much reduced total runup. Based on the
27 SUPERTANK dataset, the vertical extent of wave runup above mean water level on a
28 beach without scarp formation was found to approximately equal the significant breaking
29 wave height, H_{bs}. Therefore, a new and simple relation $R_{tw} = H_{bs}$ is proposed. The
30 linear relationship between total runup and breaking wave height is supported by a
31 conceptual derivation. In addition, the relation is extended to $U_L = R_{tw} = H_{bs}$, to
32 approximate the upper limit of beach change. This formula accurately reproduced the
33 measured upper limit of beach change from the three-dimensional experiments in the
34 Corps' Large-scale Sediment Transport Facility. For the studied laboratory cases,
35 predictions of wave runup were not improved by including a slope-dependent surf-
36 similarity parameter. The limit of wave runup was substantially less for monochromatic
37 waves than for random waves, attributed to absence of low-frequency motion.

38 ***Additional Index Words*** Beach erosion, nearshore sediment transport, wave
39 breaking, cross-shore sediment transport, physical modeling, surf zone processes.

40

41 **INTRODUCTION**

42

43 Accurate prediction of the upper limit of beach change is necessary for assessing
44 large morphologic changes induced by extreme storms. The upper limit of beach change
45 is controlled by wave breaking and the subsequent wave runup. During storms, wave
46 runup is superimposed on the elevated water level due to storm surge. WANG *et al*. (2006)
47 found the highest elevation of beach erosion induced by Hurricane Ivan in 2004 to be
48 considerably greater than the measured storm-surge level, indicating that wave runup
49 played a significant role in the upper limit of beach erosion. The limit of wave runup is
50 also a key parameter in the application of the storm-impact scale by SALLENGER (2000).
51 The Sallenger scale categorizes four levels of morphologic impact by storms through
52 comparison of the highest elevation reached by storm water (combined storm surge and
53 wave runup) and a representative elevation of the barrier island (e.g., the top of the
54 foredune ridge). Quantification of wave runup and its relationship to the upper limit of
55 morphologic change are required for understanding and predicting beach-profile changes.
56 Wave runup is composed of wave setup and swash runup, defined as a super-
57 elevation of the mean water level and fluctuation about that mean, respectively (GUZA
58 and THORNTON, 1981; HOLLAND *et al*., 1995; HOLMAN and SALLENGER, 1985; NIELSEN,
59 1988; YAMAMOTO, TANIMOTO, and HARSHINIE, 1994). Several formulas have been
60 developed to predict wave setup and runup. Based on laboratory experiments, HUNT
61 (1959) proposed various formulas estimating wave uprush, *R*, on seawalls and
62 breakwaters, and the "Hunt formula" continues in use:

63 $$\frac{R}{H} = 1.0 \frac{\tan \beta}{\sqrt{H / L_0}} \qquad (1)$$

where tan β = beach slope, H = wave height, typically taken to be the deep-water wave height, and L_0 = deepwater wavelength. HEDGES and MASE (2004) modified Hunt's original formula to include the contribution of wave setup.

BOWEN, INMAN, and SIMMONS (1968) derived a wave setup slope on a uniformly sloping beach for monochromatic waves as:

$$\frac{\partial \bar{\eta}}{\partial x} = -K \frac{\partial h}{\partial x}, \quad K = (1 + 2.67\gamma^{-2})^{-1} \tag{2}$$

where h = still-water depth, $\bar{\eta}$ = wave setup, x = cross-shore coordinate, and breaker index $\gamma = H/(\bar{\eta} + h)$. Based on both theory and laboratory measurements, BATTJES (1974) found the maximum setup under a monochromatic wave $\overline{\eta_M}$ to occur at the still-water shoreline, $\bar{\eta}_M/H_b = 0.3\gamma$, where H_b = breaking wave height. Taking the commonly used value of 0.78 for γ, the maximum setup yielded from the BATTJES formula is about 23% of the breaking wave height.

The development of most formulas predicting the limits for wave runup has involved comparisons to field measurements. Based on measurements made on dissipative beaches, GUZA and THORNTON (1981) suggested that the setup at the shoreline $\overline{\eta_{sl}}$ is linearly proportional to the significant deepwater wave height H_0:

$$\overline{\eta_{sl}} = 0.17 H_0 \tag{3}$$

In a following study, GUZA and THORNTON (1982) found the significant wave runup R_s (including both wave setup and swash runup) is also linearly proportional to the significant deepwater wave height:

$$R_s = 3.48 + 0.71 H_0 \qquad \text{(units of centimeters)} \tag{4}$$

Comparing Eqs. (3) and (4), the entire wave runup is approximately 4 times the contribution of wave setup, i.e., swash runup constitutes a significant portion, approximately 75%, of the total elevated water level. According to HUNTLEY *et al*. (1993), Eq. (4) is the best choice for predicting wave runup on dissipative beaches. Based on field measurements on highly dissipative beaches, RUESSINK, KLENHANS, and VAN DEN BEUKEL (1998) and RUGGIERO *et al.* (2001) also found linear relationships, but with slightly different empirical coefficients.

Based on field measurements, HOLMAN (1986) and several similar studies (HOLMAN and SALLENGER, 1985; RUGGIERO, HOLMAN, and BEACH, 2004; STOCKDON *et al*., 2006) argued that more accurate predictions for intermediate beaches can be obtained by including the surf similarity parameter, ξ, following the Hunt formula (Eq. 1):

$$\xi = \frac{\tan\beta}{\sqrt{H_0 / L_0}} \tag{5}$$

HOLMAN (1986) found a dependence of the 2% exceedence of runup R_2 on the deepwater significant wave height and the (offshore) surf similarity parameter:

$$R_2 = (0.83\xi + 0.2)H_0 \tag{6}$$

STOCKDON *et al*. (2006) expanded upon the HOLMAN (1986) analysis with additional data covering a wider range of beach slopes and developed the empirical equation:

$$R_2 = 1.1\left(0.35\tan\beta_f (H_0 L_0)^{\frac{1}{2}} + \frac{\left[H_0 L_0 (0.563\tan\beta_f^{\,2} + 0.004)\right]^{\frac{1}{2}}}{2}\right) \tag{7}$$

Realizing the variability of beach slope in terms of both definition and measurement, STOCKDON *et al*. (2006) defined the foreshore beach slope as the average slope over a region of two times the standard deviation of a continuous water level record.

With the exception of the original derivation by BOWEN, INMAN, and SIMMONS (1968), most predictive formulas for wave runup on a natural beach have been empirically derived based on field measurements over dissipative and intermediate beaches. Field measurements of wave runup were typically conducted with video imagery and/or resistance wire generally 5 to 20 cm above and parallel to the beach face. HOLLAND *et al*. (1995) concluded that these two measurement methods are comparable in producing accurate results.

Almost all the aforementioned field studies focused mainly on the hydrodynamics of wave runup, with little discussion on the corresponding morphologic response, particularly the upper limit of beach-profile change. Thus, in contrast to a considerable number of studies on wave runup, data are scarce that relate the limit of wave runup with the resulting beach change. In other words, the limit of beach change as related to wave runup has not been well documented.

Data from the prototype-scale laboratory experiments, including those conducted at SUPERTANK (KRAUS, SMITH, and SOLLITT, 1992; KRAUS and SMITH, 1994) and Large-scale Sediment Transport Facility (LSTF) (HAMILTON, *et al*., 2001; WANG, SMITH, and EBERSOLE, 2002), are examined in this paper to study the limit of wave runup and corresponding limit of beach or dune erosion. Specifically, this study examines 1) the levels of total wave runup, including swash runup and wave setup; 2) time-series of beach-profile change under erosional and accretionary waves; 3) the relationship between

the waves and beach-profile change; and 4) the accuracy of existing wave runup prediction methods. A new empirical formula predicting the limits of wave runup and that of beach change is proposed based on the prototype-scale laboratory data.

METHODS

SUPERTANK and LSTF Experiments

Data from two movable-bed laboratory studies, SUPERTANK and LSTF (Fig. 1), are examined to quantify the upper limits of beach-profile change, wave runup, and their relationship. Both experiments were designed to measure sediment transport and morphology change under varying prototype wave conditions. Dense instrumentation in the laboratory setting allows for well-controlled and accurate measurement of hydrodynamic conditions and morphological change. SUPERTANK was a two-dimensional wave channel with beach change induced primarily by cross-shore processes, whereas the LSTF was a three-dimensional wave basin with both cross-shore and longshore sediment transport inducing beach change.

SUPERTANK was a multi-institutional effort sponsored by the U.S. Army Corps of Engineers and conducted at the O.H. Hinsdale Wave Research Laboratory at Oregon State University from July 29 to September 20, 1991. This facility is the largest wave channel in the United States that can contain a sandy beach through which experiments comparable to the magnitude of naturally occurring waves can be conducted (KRAUS, SMITH, and SOLLITT, 1992). The SUPERTANK experiment measured total-channel hydrodynamics and sediment transport along with the resulting beach-profile change. The wave channel is 104 m long, 3.7 m wide, and 4.6 m deep (the still water level was

155 typically 1.5 m below the top during SUPERTANK) with a constructed sandy beach
156 extending 76 m offshore (Fig. 1 upper). The beach was composed of 600 m^3 of fine,
157 well-sorted quartz sand with a median size of 0.22 mm and a fall speed of 3.3 cm/s. The
158 wave generator and wave channel were equipped with a sensor to absorb the energy of
159 reflected waves (KRAUS and SMITH, 1994). The water-level fluctuations were measured
160 with 16 resistance and 10 capacitance gauges. These 26 gauges, spaced no more than 3.7
161 m apart, provided high resolution of wave propagation, especially in the swash zone.
162 The beach profile was surveyed following each 20- to 60-min wave run. The
163 initial profile was constructed based on the equilibrium beach profile developed by
164 BRUUN (1954) and DEAN (1977) as:
165 $$h(x) = Ax^{2/3} \tag{8}$$
166 where h = still-water depth, x = horizontal distance from the shoreline, and A = a shape
167 parameter, which for SUPERTANK corresponded to a median grain size of 0.30 mm.
168 The initial beach was built steeper with a greater A-value to ensure adequate water depth
169 in the offshore area (WANG and KRAUS, 2005). For efficiency, most SUPERTANK cases
170 were initiated with the final profile of the previous run. Approximately 350 profile
171 surveys were made by using an auto-tracking, infrared Geodimeter targeting prism
172 attached to a survey rod mounted on a carriage pushed by researchers. Three along-
173 channel lines were surveyed. Only the center line was analyzed in this study. Wave-
174 processing procedures are discussed in KRAUS and SMITH (1994). To separate incident-
175 band wave motion from low-frequency motion, a non-recursive, low-pass filter was
176 applied. The period cutoff for the filter was set to twice the peak period of the incident
177 waves.

The LSTF is a three-dimensional wave basin located at the U.S. Army Corps of Engineers Coastal and Hydraulic Laboratory in Vicksburg, Mississippi. Operation procedures are discussed in HAMILTON *et al*. (2001). The LSTF was designed to study longshore sediment transport (WANG, *et al.*, 2002; WANG, SMITH, and EBERSOLE, 2002). The LSTF is capable of generating wave conditions comparable to the naturally occurring wave heights and periods found along low-energy open coasts and bays. The LSTF has dimensions of 30 m across-shore, 50 m longshore, with walls 1.4 m high (Fig. 1 lower). The beach was designed in a trapezoidal plan shape composed of approximately 150 m^3 of very well sorted fine quartz sand with a median grain size of 0.15 mm and a fall speed of 1.8 cm/s. Initial construction of the beach was also based on the equilibrium profile (Eq. 8). The beach profile was surveyed using an automated bottom-tracking profiler capable of resolving bed ripples. The beach was typically replenished after 3 to 9 hours of wave activity. Long-crested and unidirectional irregular waves with a relatively broad spectral shape were generated at a 10 deg incident angle in the horizontal section of the basin. The wave height and peak wave period were measured with capacitance wave gauges sampling at 20 Hz, statistical wave properties were calculated by spectral analysis. The experimental procedures in LSTF are described in WANG, SMITH, and EBERSOLE (2002).

Data Analysis

Although the entire SUPERTANK dataset is available, five cases with a total of 30 wave runs were selected from the 20 initial cases. The selection was based on the particular purpose of the wave run, the trend of net sediment transport, and the beach

response. Time-series of beach-profile change, cross-shore distribution of wave height, and mean water level were analyzed. Scarp presence was also identified. The upper limits U_L for the non-scarped beach profile runs were identified based on the upper profile convergence point, above which no beach change occurred. The upper limit identified for the scarped runs was at the elevation of the scarp toe. The other location examined was the lower limit of beach change L_L. The lower limit, or lower profile convergence point, was identified at the depth contour below which no change occurred.

For the 30 SUPERTANK wave runs examined, the water level and zero-moment wave height were analyzed. From the cross-shore wave height distribution (or wave-energy decay), the breaker point H_b was defined at the location with a sharp decrease in wave height (WANG *et al*., 2002). The total wave runup R_{tw} was defined by the location and beach elevation of the swash gauge that contained a value larger than zero wave height, i.e., water reached that particular gauge. The above procedure did not involve any statistical analysis, but rather was determined by the measurements available from SUPERTANK. Hence, there may be some differences between the R_{tw} determined in this study and the 2% exceedence of runup ($R_{2\%}$) as appears in some predictive equations, obtained from video (e.g., HOLLAND *et al*., 1995) and horizontally elevated wires (e.g., GUZA and THORNTON, 1982).

Two LSTF experiments, one conducted under random spilling breaker waves and one under random plunging breaker waves, were examined in this study. The LSTF data were examined for the upper limit of beach change. The beach-profiles analyzed here were surveyed through the middle of the basin. The maximum runup was not directly

measured due to the lack of swash gauges. The main objective of the LSTF analysis was to apply the SUPERTANK results to a three-dimensional beach.

RESULTS

Overall, 30 SUPERTANK wave runs and two LSTF wave cases were analyzed (Table 1). The two LSTF cases, under a spilling and a plunging breaker, examined the effect of the breaker types on sediment transport and the resulting beach-profile change. The thirty SUPERTANK wave runs are composed of twelve erosional random wave runs, three erosional monochromatic wave runs, seven accretionary random wave runs, three accretionary monochromatic wave runs, and five dune erosion random wave runs. In Table 1, the first two numbers in the wave run ID "10A_60ER" indicate the major data collection case, the letter "A" indicates a particular wave condition, and the numerals indicate the duration of wave action in minutes. The notation used in Table 1 and in all equations is listed in Appendix I. The erosional and accretionary cases were designed based on the Dean number N,

$$N = \frac{H_{bs}}{wT} \tag{9}$$

where H_{bs} = significant breaking wave height; w = fall speed of the sediment, and T = wave period (KRAUS, SMITH, and SOLLITT, 1992).

Beach-Profile Change

245 Analysis of the time-series of beach-profile change for the SUPERTANK
246 experiment can be found in ROBERTS, WANG, and KRAUS (2007). The first
247 SUPERTANK wave run, ST_10A, was conducted with a monotonic initial profile (Eq.
248 8). Figure 2 illustrates four time-series beach-profiles surveyed at initial, 60, 130, and
249 270 min. The design wave conditions are included as an inset in the figures, where H_{mo}
250 is the zero-moment wave height, T_p is the peak spectral wave period, and n is spectral
251 peakedness. Significant beach-profile change occurred with substantial shoreline
252 recession, along with the development of an offshore bar. Initially, the foreshore
253 exhibited a convex shape while the end profile was concave. The upper limit of beach-
254 profile change was measured at 0.66 m above mean water level (MWL) for all three time
255 segments. An apparent point of profile convergence was measured at the 1.35 m depth
256 contour, beyond which profile elevation change cannot be clearly identified.
257 The subsequent wave runs were conducted over the final profile of the previous
258 wave run, i.e., over a barred beach. The beach-profile changes are detectable, but much
259 more subtle than the initial run (Fig. 2), especially for the accretionary wave runs with
260 lower wave heights. Figure 3 shows an example of an accretionary wave run, ST_30A.
261 The upper limit was determined to be at 0.31 m above MWL (Fig. 3 lower). One of the
262 surveys (60 min) exhibited some changes above that convergence level; however these
263 changes may be attributable to survey error. The offshore-profile convergence point was
264 determined at a depth contour of around 1 m.
265 A scarp developed in some of the erosional wave runs (Fig. 4). The scarp was
266 induced by wave erosion of the base of the dune or the dry-beach, subsequently causing
267 the overlying sediment to become unstable and collapse. The resulting beach slope

268 directly seaward of the scarp tends to be steeper than on a non-scarped beach. The upper
269 limit of beach change is apparently at the top of the scarp, controlled by the elevation of
270 the beach berm or dune, and does not necessarily represent the vertical extent of wave
271 action. The upper limit of beach change in this study was selected at the base of the near-
272 vertical scarp, measured at 0.31 m above MWL during ST_60A (Fig. 4). Therefore, for
273 the scarped case, the upper limit was controlled by both wave action and gravity-driven
274 dune collapse. Little beach-profile change was observed offshore.

275 SUPERTANK experiments also included several runs with monochromatic waves.
276 Beach-profile change under monochromatic wave action was substantially different from
277 those under the more realistic random waves (Fig. 5). The monochromatic waves tended
278 to create erratic and undulating profiles. For ST_I0, the upper limit of beach-profile
279 change was estimated at around 0.50 m and varied slightly during the different wave runs.
280 The erratic profile evolution did not seem to approach a stable equilibrium shape, and it
281 did not have an apparent profile convergence point. In addition, the profile shape
282 developed under monochromatic waves does not represent profiles typically measured in
283 the field (WANG and DAVIS, 1998). This implies that morphological change measured in
284 movable-bed laboratory experiments under monochromatic waves may not be applicable
285 to a natural setting.

286 Similar analyses were also conducted for the data from the LSTF. The waves
287 generated in the LSTF had smaller heights and shorter periods as compared to the
288 SUPERTANK waves. Two cases with distinctively different breaker types, one spilling
289 and one plunging, were examined.

290 The spilling wave case was initiated with the Dean equilibrium beach profile (Eq.
291 8). Because of the smaller wave heights, beach-profile change occurred at a slower rate.
292 Similar to the first SUPERTANK wave run, ST_10A, a subtle bar formed over the initial
293 monotonic beach profile (Fig. 6 upper). For the spilling wave case, the upper limit of
294 beach change was 0.23 m above MWL, as identified from the smaller scale plot (Fig. 6
295 lower). The profile converges on the seaward slope of the offshore bar. For the LSTF
296 plunging wave case, shoreline advance occurred with each wave run along with sustained
297 onshore migration of the bar (Fig. 7). The accumulation at the shoreline was subtle, but
298 can be identified if viewed locally (Fig. 7 lower). The upper limit of beach-profile
299 change was located at 0.26 m above MWL, with the lower limit identified at the profile
300 convergence point midway on the seaward slope of the bar. Overall, the trends observed
301 in the three-dimensional LSTF experiment are comparable to those in the two-
302 dimensional SUPERTANK experiment.
303 Table 2 summarizes the upper and lower limits of change during each wave run,
304 including the breaking wave height. In summary, for the 30 SUPERTANK wave runs
305 and two LSTF wave cases, the incident breaking wave height ranged from 0.26 to 1.18 m
306 (Table 2). The measured upper limit of profile change, including the scarped dune cases,
307 ranged from 0.23 to 0.70 m. The lower limit of beach change ranged from 0.50 to 1.61 m
308 below MWL. Relationships between the profile change and wave conditions are
309 discussed in the following sections.
310

311 **Cross-shore Distribution of Wave Height**

312 Wave-height decay is representative of the energy dissipation as a wave
313 propagates onshore. Wave decay patterns were measured by the closely spaced gauges
314 for both the SUPERTANK and the LSTF experiments. Figure 8 shows time-series wave
315 decay patterns measured at the first SUPERTANK wave run, ST_10A. As discussed
316 above, considerable beach profile change, for example the formation of an offshore bar,
317 was produced during this wave run (Fig. 2). The substantial morphology change also
318 influenced the pattern of wave decay. The point of steep wave decay migrated slightly as
319 the beach morphology changed from the initial monotonic profile to a barred-beach
320 profile. This point was defined as the location and height at which the wave breaks
321 (WANG *et al*., 2002). For ST_10A, the significant breaking wave height was 0.68 m.
322 The rate of wave-height decay tended to be smaller in the mid-surf zone (10 to 20 m) as
323 compared to the breaker zone (20 to 25 m) and the inner surf zone (landward of 10 m).
324 The offshore wave height remained largely constant until reaching the breaker line.
325 The wave decay pattern for the longer period accretionary wave run, ST_30A (Fig.
326 9), was considerably different than the steep erosive waves. The significant breaking
327 wave height was 0.36 m. The time-series wave pattern remained constant for each wave
328 run, apparently not influenced by the subtle morphology change (Fig. 3). The bar was
329 formed during the previous wave runs with greater wave heights. Therefore, instead of
330 breaking over the bar, shoaling or increase in height of the long period wave was
331 measured (at around 30 m). The main breaker line was identified at around 15 m, where
332 a sharp drop in wave height was observed.

For the dune erosion run, ST_60A, the wave height remained largely constant offshore (Fig. 10). Significant wave-height decay was measured over the offshore bar at approximately 30 m, with a breaker height of 0.61 m. A noticeable increase in wave height was measured at around 15 m offshore, likely a result of reflected waves off the scarp, followed by a sharp decrease in height in the inner surf zone.

The cross-shore distribution of wave height for the monochromatic wave run ST_I0 was erratic with both temporal and spatial irregularity (Fig. 11). The erratic wave height distribution corresponds to the irregular beach-profile change observed during this wave run (Fig. 5). The breaking wave height varied considerably, from 0.72 to 0.81 m, likely caused by reflection of the monochromatic waves from the beach face. The wave-height variation in the offshore region, seaward of the breaker line around 30 m, was likely related to oscillations in the wave tank.

The LSTF experiments were designed to examine the effects of different breaker types on sediment transport and morphology change. Offshore wave heights of 0.27 m were generated for both cases (Fig. 12), which had different wave periods. However, the cross-shore distribution of wave heights was considerably different. The wave-height decay at the breaker line was much greater for the plunging case than for the spilling case, as expected. The breaking wave height was 0.26 m and 0.27 m for the spilling and plunging wave runs, respectively.

Wave Runup

The extent and elevation of wave runup for the SUPERTANK experiments were measured directly by the closely spaced swash gauges (KRAUS and SMITH, 1994). Figure

13 shows the cross-shore distribution of time-averaged water level and wave runup for the erosive wave run, ST_10A. The swash zone water level was measured by the discrete swash gauges, as discussed above, and does not represent time-averaged water level. Elevated water levels were measured in the surf zone. As expected, the mean water level in the offshore area remained around zero. It is necessary to separate the elevation caused by wave setup and swash runup. An inflection point (labeled with an arrow and "ip") can be identified from the cross-shore distribution curve of the mean water level (Fig. 13). The inflection point also tends to occur around the still-water shoreline and is regarded here as the distinction between wave setup and swash runup. For this run, the setup measured at the still-water shoreline was 0.1 m, which is about 17 percent of the total wave runup of 0.6 m.

For the accretionary wave run, ST_30A, the inflection point in the mean-water level also occurs around the still-water shoreline (Fig. 14). The average setup at the shoreline was approximately 0.07 m, also about 17 percent of the total wave runup of 0.4 m. Total wave runup was significantly limited by the vertical scarp as shown in the dune erosion run of ST_60A (Fig. 15). A broad setdown was measured just seaward of the main breaker line. The inflection point of the cross-shore distribution of the mean water level occurred between 10 and 11 m, before reaching the still-water shoreline at 8 m. The setup measured at the inflection point at 11 m was approximately 0.03 m. The wave setup contributed 18 percent of the total wave runup of 0.17 m, similar to the above two cases.

The cross-shore distribution of time-averaged mean water level and wave runup for ST_I0 (monochromatic waves) was erratic (Fig. 16). As opposed to the irregular

wave cases, a zero mean-water level was not measured at a considerable number of offshore wave gauges. In addition, significant variances among different wave runs were also measured. The total wave runup varied from 0.16 to 0.35 m, with an average of 0.26 m. The inflection point in the mean-water level distribution occurs around the still-water shoreline at 5 m. The maximum setup at the still-water shoreline was 0.08 m, which is 31 percent of the total wave runup. The smaller contribution of the swash runup to the total wave runup can be attributed to the lack of low-frequency motion in the monochromatic waves.

DISCUSSION

Relationship between Wave Runup, Incident Wave Conditions, and Limit of Beach Profile Change

The measured breaking wave height, upper limit of beach-profile change, and total wave runup from the SUPERTANK experiments are compared in Figure 17. The thirty runs examined are divided into three categories describing non-scarped random wave runs, scarped random wave runs, and monochromatic wave runs. For the 16 non-scarped random wave runs, except the three runs (10B_20ER, 10E_270ER and 30D_40AR), the elevations of wave runup and upper limit of beach change roughly equal the significant breaking wave height. All three outliers had relatively lower measured swash runup. The discrepancy may be caused by the performance of the capacitance gauge. The partially buried capacitance gauges in the swash zone required the sand to be fully saturated (KRAUS and SMITH, 1994). Both 10B_20ER and 30D_40AR are initial

short-duration runs, during which the sand may not have been fully saturated. However this does not explain the discrepancy for 10E_270ER, with cause unknown.

For the scarped random wave runs, the breaking wave height was much greater than the elevation of wave runup, which was limited by the vertical scarp. Because the upper limit of beach change was identified at the toe of the scarp, a relationship among the breaker height, wave runup, and beach-profile change is not expected for the scarped random wave runs. The much lower wave runup by monochromatic waves as compared to the breaker height was likely caused by the lack of low-frequency motion. No relationship could be found among the three parameters for monochromatic waves.

Based on the above observations from the SUPERTANK data with breaking wave heights ranging from 0.4 to 1.2 m (Fig. 17), a simple relationship between the measured wave runup height on a non-scarped beach and the breaker height is found:

$$R_{tw} = 1.0 H_{bs} \tag{10}$$

The average ratio of R_{tw} over H_{bs} for the 16 non-scarped wave runs was 0.93, with a standard error on the mean of 0.05. Excluding the three questionable measurements, 10B_20ER, 10E_270ER and 30D_40AR, the average R_{tw}/H_{bs} was 1.01, with a standard error of 0.02. To be conservative because of limited data coverage, a value of 1.0 was assigned in Eq. (10). Caution should be exercised in applying Eq. (10) to higher waves than the range examined here.

Comparisons of the measured wave runup with the various existing empirical formulas (Eqs. 4, 6, and 7) and Eq. (10) are summarized in Figure 18 and Table 3. It is recognized that Eq. (4) predicts significant runup height, whereas Eqs. (6) and (7) predict 2% exceedence of runup. The measured runup R_{tw} from SUPERTANK represents a

maximum value of total wave runup (Eq. 10). As shown in Fig. 18, previous formulas did not reproduce the measured wave runup at SUPERTANK. For the 16 non-scarped wave runs, 81% of the predictions from Eq. (10) fall within 15% of the measured wave runup. In contrast, for Eqs. (4), (6) and (7), only 25%, 6% and 13% of the predictions, respectively, fall within 15% of the measured values. Eqs. (6) and (7) under-predicted the measured wave runup significantly for the erosional cases, but over-predicted runup for the accretionary wave cases. The discrepancy is caused by the substantially greater value of ξ for the gentle long-period accretionary waves than for the steep short-period erosional waves (Table 1). Agreement between measured and predicted values was reduced by including the surf similarity parameter, ξ. The simpler Eq. (4) developed by GUZA and THORNTON (1982) based only on the offshore wave height, more accurately reproduced the measured values of wave runup than Eqs. (6) and (7).

Equation (10) was applied to the three-dimensional LSTF experiments with lower wave heights than in SUPERTANK. Although wave runup was not directly measured in the LSTF experiments, it is assumed here that the total runup is equal to the upper limit of beach-profile change, a reasonable assumption as verified by the SUPERTANK data. For the spilling wave case, taking the upper limit of beach change at 0.23 m as the value for total wave runup, the breaking wave height of 0.26 m resulted in an over-prediction of 13%. For the plunging wave case, the upper limit of beach change was 0.26 m, which is almost equal to the 0.27 m breaking wave height. Therefore, the LSTF data, with a finer grain size (0.15 mm) than SUPERTANK (0.22 mm), support the new predictive equation (Eq. 10).

448 The dependence of wave runup on beach slope has been questioned by various
449 studies. DOUGLASS (1992) re-analyzed the HOLMAN (1986) dataset underlying
450 development of Eq. (6) and stated that runup and beach-face slope are not well correlated.
451 DOUGLASS argued that beach slope is a dependent variable that is free to respond to the
452 incident waves and should not be included in runup prediction. SUNAMURA (1984) and
453 KRIEBEL, KRAUS, and LARSON (1991) found dependencies of beach slope on wave height
454 and period, the latter reference giving a predictive formula expressed in terms of the
455 Dean number (Eq. 9). NIELSEN and HANSLOW (1991) found a relationship between the
456 surf similarity parameter and runup on steep beaches. However, for gentle beaches with
457 slopes less than 0.1, they suggested that the surf similarity parameter was not related to
458 runup. A subsequent study by HANSLOW and NIELSON (1993) conducted on dissipative
459 beaches of Australia found that maximum setup did not depend on beach slope.
460 In practice, beach face slope is a difficult parameter to define and determine.
461 Except for STOCKDON *et al*. (2006), a clear definition of beach slope is not given in most
462 studies. STOCKDON *et al*. defined the foreshore beach slope as the average slope over a
463 region of two times the standard deviation of a continuous water-level record. In
464 predictive modeling of morphology change, relations between runup and foreshore slope
465 would be interdependent. In the present study, the slope was defined over the portion of
466 the beach extending roughly 1 m landward and seaward from the shoreline. Substantially
467 different beach slopes can be obtained by imposing different definitions. Inclusion of the
468 beach slope in predictive relations for wave runup thus adds ambiguity in applying such
469 formulations.

Determining offshore wave height may also introduce uncertainty. In most field studies, the offshore wave height is taken to be the measurement at a wave gauge in the study area. Similarly, in this study it is taken as the wave height measured at the farthest offshore gauge. The definition of an offshore wave height varies between studies, in which it is often taken at whatever depth the instrument is deployed (GUZA and THORNTON, 1981; GUZA and THORNTON, 1982; HOLMAN, 1986). In addition, under storm conditions, estimation of the offshore wave height may not be straightforward (WANG *et al*. 2006).

A Conceptual Derivation of the Proposed Wave Runup Model

Swash uprush on a sloping beach is often approximated using a ballistics approach of bore propagation (BALDOCK and HOLMES, 1999; COCO, O'HARE, and HUNTLEY, 1999; LARSON, KUBOTA, and ERIKSON, 2004; MASE, 1988; SUHAYDA, 1974). Most derivations are based on the bore runup model of SHEN and MEYER (1963) and the radiation stress formulation of LONGUET-HIGGENS and STEWART (1962). In the following derivation, a similar approach is adopted to examine the physics foundation of Eq. (10).

Assuming a normally incident wave and neglecting longshore variations, the forces acting on a water element in the swash zone in the cross-shore direction, *x*, (Fig. 19) can be balanced as:

$$-\rho g \Delta x \Delta y \Delta z \sin\beta - \frac{f}{8}\rho \Delta x \Delta y V_x^{\,2} = \rho \Delta x \Delta y \Delta z \frac{\partial V_x}{\partial t} \qquad (11)$$

where, ρ = density of water; g = acceleration due to gravity; Δx, Δy, and Δz, = length, width, and height, of the water element, respectively; sin β = beach slope; f = friction coefficient; and V_x = velocity. Eq. (11) can be reduced to

$$\frac{\partial V_x}{\partial t} = -g \sin\beta - \frac{f}{8\Delta z} V_x^2 \tag{12}$$

Assuming the friction force is negligible, an assumption supported by experiments discussed in KOMAR (1998), Eq. (12) is further reduced to

$$\frac{\partial V_x}{\partial t} = -g \sin\beta \tag{13}$$

Influences of friction and infiltration on swash motion are discussed in PULEO and HOLLAND (2001). Integrating Eq. (13) with respect to time, yields

$$V_x = V_o - gt \sin\beta \tag{14}$$

where, V_o = initial velocity. Integrating Eq. (14) again with respect to time gives the swash excursion, x, as a function of time, t:

$$x(t) = V_o t - \frac{gt^2}{2} \sin\beta \tag{15}$$

From Eq. (14), the maximum uprush occurs at a time, t_{max}, when the velocity becomes zero:

$$t_{max} = \frac{V_o}{g \sin\beta} \tag{16}$$

with a corresponding value of maximum swash excursion of

$$x(t_{max}) = \frac{V_o^2}{2g \sin\beta} \tag{17}$$

Assuming a small and planar foreshore slope, then tan $\beta \approx$ sin β, and the elevation of the maximum swash uprush R_{sr_max},becomes:

512 $$R_{sr\_\max} = x(t_{\max})\tan\beta = \frac{V_o^2}{2g\sin\beta}\tan\beta \approx \frac{V_o^2}{2g} \quad (18)$$

513 Eq. (18) suggests that the maximum elevation of swash runup is not a function of beach
514 slope if bottom friction forcing is neglected.

515 The initial velocity V_o can be approximated by the velocity of the wave, C. In
516 shallow water, the wave velocity is limited by the local water depth, h_l.

517 $$V_o \approx C = \sqrt{gh_l} \quad (19)$$

518 Assuming a linear relationship between local breaking or brreaking wave height, H_{bl}, and
519 the water depth, h_l

520 $$H_{bl} = \gamma h_l \quad (20)$$

521 where γ = the breaker index. Eq. (19) then becomes

522 $$V_o^2 \approx C^2 = g\frac{H_{bl}}{\gamma} \quad (21)$$

523 Substituting Eq. (21) into Eq. (18)

524 $$R_{sr\_\max} = \frac{V_o^2}{2g} = \frac{gH_{bl}}{2g\gamma} = \frac{H_{bl}}{2\gamma} \quad (22)$$

525 Because of wave height to depth scaling in the surf zone, it is reasonable to assume that
526 the initial velocity V_o can be taken at the main breaker line. With significant breaker
527 height H_{bs} Eq. (22) then becomes

528 $$R_{sr\_\max} = \frac{H_{bs}}{2\gamma} = \alpha H_{bs} \quad (23)$$

529 where $\alpha = 1/2\gamma$. Eq. (23) indicates a linear relationship between breaking wave height
530 and the maximum swash runup, supporting the findings deduced from the SUPERTANK
531 experiment.

KAMINSKY and KRAUS (1994) examined a large dataset on breaking wave criteria that included both laboratory and field measurements, They found the majority of γ values range from 0.6 to 0.8, which yields α values from 0.63 to 0.83. Based on previous discussion (Figs. 13 through 16), swash runup constitutes approximately 83% of the total wave runup. Adding the 17% contribution from the wave setup, the total wave runup R_{tw} is roughly equal to the breaking wave height, further supporting the predictive equation developed from the SUPERTANK dataset. Thus, the empirical model of total wave runup developed based on the SUPERTANK data is supported by an accepted physical picture. In addition, little ambiguity exists in the straight-forward parameterization as given in Eq. 10.

CONCLUSIONS

The SUPERTANK data set indicates that the vertical extent of wave runup above mean water level on a non-scarped beach is approximately equal to the significant breaking wave height. A simple formula for predicting the total wave runup $R_{tw} = 1.0\ H_{bs}$ was developed by comparison to measurements and justified by a derivation based on ballistic theory of swash motion. This formula does not include beach slope, which is difficult to measure and is itself dependent on wave properties. The new model was applied to the three-dimensional LSTF experiments and accurately reproduced the measured wave runup. Inclusion of the slope-dependent surf similarity parameter decreased the accuracy of the calculated wave runup as compared to the measured values.

An exception to the direct relationship between breaking wave height and runup concerns the presence of dune or beach scarping. The steep scarp substantially limits the

555 uprush of swash motion, resulting in a much reduced maximum level, as compared with
556 the non-scarping cases. For monochromatic waves, the measured wave runup was much
557 smaller than the breaking wave height. The lack of low-frequency modulation limits the
558 wave runup for monochromatic waves.

559 Based on the SUPERTANK and LSTF experiments, the upper limit of beach-
560 profile change was found to be approximately equal to the total vertical excursion of
561 wave runup. Therefore, the breaking wave height can be used to provide a reliable
562 estimate of the limit of wave runup which, in turn, can serve as an approximation of the
563 landward limit of beach change: $U_L = R_{tw} = H_{bs}$. Physical situations that are exceptions
564 to this direct relationship are beaches with beach or dune scarps. For the scarped cases,
565 the upper limit of beach change was much higher than the total swash runup and was
566 controlled by the elevation of the berm or dune.

567

568

569 **ACKNOWLEDGEMENTS**

570 This study is jointly funded by the Coastal Inlet Research Program (CIRP) at the
571 U.S Army Engineer Research and Development Center and the University of South
572 Florida. Constructive reviews by Dr. Nicole Elko and two anonymous reviewers are
573 acknowledged.

574

575

576 **APPENDIX I - NOTATION**

577

578 *The following symbols are used in this paper:*

579 A shape parameter relating to grain size and fall velocity
580 C wave velocity
581 f friction coefficient

582	g	gravitational acceleration
583	h	still-water depth
584	H	wave height
585	H_b	breaking wave height
586	H_{bl}	local breaking wave height
587	H_{bs}	significant breaking wave height
588	H_{b_h}	high frequency component of wave height at the breaker line
589	H_{b_l}	low frequency component of wave height at the breaker line
590	h_l	local water depth
591	H_o	significant deepwater wave height
592	H_{sl_h}	high frequency component of wave height at the shoreline line
593	H_{sl_l}	low frequency component of wave height at the shoreline line
594	L_L	lower limit of beach change
595	L_0	deepwater wavelength
596	n	spectral peakedness parameter
597	N	Dean number
598	R_s	significant wave runup
599	R_{sr_max}	elevation of maximum swash uprush
600	R_{tw}	total wave runup
601	R_2	2% exceedence of runup
602	T	wave period
603	t_{max}	time of maximum swash excursion
604	T_p	peak spectral wave period
605	U_L	upper limit of beach change
606	V_o	initial velocity
607	V_x	velocity of a water particle in the across shore
608	w	sediment fall velocity
609	x	cross-shore coordinate; horizontal distance from the shoreline
610	$\tan\beta$	beach slope
611	$\tan\beta_f$	foreshore beach slope
612	γ	breaker index
613	Δx	length of a water particle
614	Δy	width of a water particle
615	Δz	height of a water particle
616	$\overline{\eta}$	wave setup
617	$\overline{\eta_M}$	wave setup under monochromatic waves
618	$\overline{\eta_{sl}}$	wave setup at the shoreline
619	ξ	surf-similarity parameter
620	ρ	water density
621		

622

623 **LITERATURE CITED**

BALDOCK, T.E. and HOLMES, P., 1999. Simulation and prediction of swash oscillation on a steep beach. *Coastal Engineering*, 36, 219-242.

BATTJES, J.A., 1974. Computations of set-up, longshore currents, run-up overtopping due to wind-generated waves. *Report, 74-2*, Delft Univ. Technol., Delft, The Netherlands.

BOWEN, A.J., INMAN, D.L., and SIMMONS, V.P., 1968. Wave "set-down" and "set-up." *Journal of Geophysical Research*, 73(8), 2569-2577.

BRUUN, P., 1954. Coastal erosion and the development of beach profiles. *Technical Memo., No. 44*, Beach Erosion Board, U.S. Army Corps of Engineers.

COCO, G., O'HARE, T.J., and HUNTLEY, D.A., 1999. Beach Cusps: A comparison of data and theories for their formation. *Journal of Coastal Research*, 15(3), 741-749.

DEAN, R.G., 1977. Equilibrium beach profiles: U.S. Atlantic and Gulf coasts. *Ocean Engineering Report*, No. 12, Dept. of Civil Eng., Univ. of Delaware, Newark, DE.

DOUGLASS, S.L**.,** 1992. Estimating extreme values of run-up on beaches. *Journal of Waterway, Port, Coastal and Ocean Engineering*, 118, 220-224.

GUZA, R.T. and THORNTON, E.B., 1981. Wave set-up on a natural beach. *Journal of Geophysical Research*, 86(C5), 4133-4137.

GUZA, R.T. and THORNTON, E.B., 1982. Swash oscillations on a natural beach. *Journal of Geophysical Research*, 87(C1)**,** 483-490.

HAMILTON, D.G., EBERSOLE, B.A., SMITH, E.R., and WANG, P., 2001. Development of a large-scale laboratory facility for sediment transport research. *Technical Report*,

ERDC/SCH-TR-01-22, U.S. Army Engineer Research and Development Center, Vicksburg, Mississippi.

HAMILTON, D.G. and EBERSOLE, B.A., 2001. Establishing uniform longshore currents in a large-scale laboratory facility. *Coastal Engineering*, 42, 199-218

HANSLOW, D. and NIELSEN, P., 1993. ,Shoreline set-up on natural beaches. *Journal of Coastal Research, SI* 15, 1-10.

HEDGES, T.S., and MASE, H., 2004. Modified Hunt equation incorporating wave setup. *Journal of Waterway, Port, Coastal and Ocean Engineering*, 109-113.

HOLLAND, K.T., RAUBENHEIMER, B., GUZA, R.T., and HOLMAN, R.A., 1995. Runup kinematics on a natural beach. *Journal of Geophysical Research*, 100(C3), 4985-4993.

HOLMAN, R.A., 1986. Extreme value statistics for wave run-up on a natural beach. *Coastal Engineering*, 9, 527-544.

HOLMAN, R.A. and SALLENGER, A.H., 1985. Setup and swash on a natural beach. *Journal of Geophysical Research*, 90(C1), 945-953.

HUNT, I.A. JR., 1959. Design of seawalls and breakwaters. *Journal of the Waterways and Harbors Division*, 83(3), 123-152.

HUNTLEY, D.A., DAVIDSON, M., RUSSELL, P., FOOTE, Y., and HARDISTY, J., 1993. Long waves and sediment movement on beaches: Recent observations and implications for modeling. *Journal of Coastal Research*, 15, 215-229.

KAMINSKY, G. and KRAUS, N.C., 1994. Evaluation of depth-limited breaking wave criteria. *Proceedings of Ocean Wave Measurement and Analysis, Waves '94*, New York: ASCE Press, 180-193.

669 KOMAR, P.D., 1998. *Beach Processes and Sedimentation*. New Jersey: Prentice Hall,
670 544p.
671 KRAUS, N.C. and SMITH, J.M., (Eds.) 1994. SUPERTANK Laboratory Data Collection
672 project, Volume 1: Main text. *Technical Report CERC-94-3*, U.S. Army Eng.
673 Waterways Experiment Station, Coastal Eng.. Res. Center, Vicksburg, MS.
674 KRAUS, N.C., SMITH, J.M., and SOLLITT, C.K., 1992. SUPERTANK Laboratory data
675 collection project. *Proceedings 23rd Coastal Engineering Conference*, ASCE,
676 2191-2204.
677 KRIEBEL, D.L., KRAUS, N.C., and LARSON, M., 1991. Engineering methods for
678 predicting beach profile response. *Proceedings of Coastal Sediments '91¸ASCE,*
679 *557-571*.
680 LARSON, M.; KUBOTA, S., and ERIKSON, L., 2004. Swash-zone sediment transport and
681 foreshore evolution: field experiments and mathematical modeling. *Marine*
682 *Geology*, 212(1–4), 61–79.
683 LONGUET-HIGGINS, M.S. and STEWART, R.W., 1962. Radiation stress and mass transport
684 in gravity waves, with application to "Surf Beat." *Journal of Fluid Mechanics*,
685 13, 481-504.
686 MASE, H., 1988. Spectral characteristics of random wave run-up. *Coastal Engineering*,
687 12**,** 175-189.
688 NIELSEN, P., 1988. Wave setup: A field study. *Journal of Geophysical Research*,
689 93(C12), 15,643-652.
690 NIELSEN, P. and HANSLOW, D.J., 1991. Wave runup distributions on natural beaches.
691 *Journal of Coastal Research*, **7** (4), 1139-1152.

692 PULEO, J.A. and HOLLAND, K.T., 2001. Estimating swash zone friction coefficients on a
693 sandy beach. *Coastal Engineering,* 43, 25-40.

694 ROBERTS, T.M., WANG, P., and KRAUS, N.C., 2007. Limits of beach and dune erosion in
695 response to wave runup elucidated from SUPERTANK. *Proceedings of Coastal*
696 *Sediments '07*, ASCE, 1961-1973.

697 RUESSLINK, B.G., KLEINHANS, M.G., and VAN DEN BEUKEL, P.G.L., 1998. Observations
698 of swash under highly dissipative conditions, *Journal of Geophysical Research*,
699 103, 3111–3118.

700 RUGGIERO, P., HOLMAN, R.A., and BEACH, R.A**.,** 2004. Wave run-up on a high-energy
701 dissipative beach. *Journal of Geophysical Research*, 109(C06025), 1-12.

702 RUGGIERO, P., KOMAR, P.D., MCDOUGAL, W.G., MARRA, J.J., and BEACH, R.A., 2001.
703 Wave runup, extreme water levels and the erosion of properties backing beaches.
704 *Journal of Coastal Research*, 17 (2), 407-419.

705 SALLENGER, A.H., 2000. Storm impact scale for barrier island. *Journal of Coastal*
706 *Research,* 16, 890-895.

707 SHEN, M.C. and MEYER, R.E., 1963. Climb of a bore on a beach 3: run-up. *Journal of*
708 *Fluid Mechanics,* 16, 113-125.

709 STOCKDON, H.F., HOLMAN, R.A., HOWD, P.A., and SALLENGER, A.H., 2006. Empirical
710 parameterization of setup, swash, and runup. *Coastal Engineering*, 53, 573-588.

711 SUHAYDA, J.N., 1974. Standing waves on beaches. *Journal of Geophysical Research,*
712 79(21)**,** 3065-3071.

713 SUNAMURA, T., 1984. Quantitative prediction of beach-face slopes. *Geological Society*
714 *of America Bulletin*, 95,242-245.

WANG, P., EBERSOLE, B.A., SMITH, E.R., and JOHNSON, B.D., 2002. Temporal and special variations of surf-zone currents and suspended-sediment concentration. *Coastal Engineering*, 46, 175-211.

WANG, P. and DAVIS, R.A. JR., 1998. A beach profile model for a barred coast – case study from Sand Key, west-central Florida. *Journal of Coastal Research*, 14, 981-991.

WANG, P. and KRAUS, N.C., 2005. Beach profile equilibrium and patterns of wave decay and energy dissipation across the surf zone elucidated in a large-scale laboratory experiment. *Journal of Coastal Research*, 21, 522-534.

WANG, P., KIRBY, J.H., HABER, J.D., HORWITZ, M.H., KNORR, P.O., and KROCK, J.R., 2006. Morphological and sedimentological impacts of Hurricane Ivan and immediate post-storm beach recovery along the northwestern Florida barrier-island coasts, *Journal of Coastal Research*, 22(6), 1,382-1,402.

WANG, P., SMITH, E.R. and EBERSOLE, B.A., 2002. Large-scale laboratory measurements of longshore sediment transport under spilling and plunging breakers. *Journal of Coastal Research,* 18, 118-135.

YAMAMOTO, Y., TANIMOTO, K., and HARSHINIE, K.G., 1994. Run-up of irregular waves on gently sloping beach. *Proceedings 23rd Coastal Engineering Conference*, ASCE, 689-703.

FIGURES

Figure 1. The SUPERTANK experiment (upper) and LSTF (lower) during wave runs.

Figure 2. The first SUPERTANK wave run, ST_10A erosional case. Substantial shoreline erosion occurred on the initial monotonic profile with the development of an offshore bar. The horizontal axis “distance” refers to the SUPERTANK coordinate system and is not directly related to morphological features.

Figure 3. The SUPERTANK ST_30A accretionary wave run. There was subtle beach face accretion, with an onshore migration of the offshore bar (upper). The accretion near the shoreline is identified if viewed at local scale (lower).

Figure 4. The SUPERTANK ST_60A dune erosion wave run. A nearly vertical scarp developed after 40 min of wave action, with the upper limit of beach change identified at the toe of the dune scarp.

Figure 5. The SUPERTANK ST_I0 accretionary monochromatic wave run. The resulting beach-profile under monochromatic waves is erratic and undulating.

Figure 6. The LSTF spilling wave case. Erosion occurred in the foreshore and inner surf zone. The eroded sediment was deposited on an offshore bar.

Figure 7. The LSTF plunging wave case. Slight foreshore accretion and landward migration of the offshore bar occurred during the wave run.

Figure 8. Cross-shore wave-height distribution measured during SUPERTANK ST_10A.

Figure 9. Cross-shore wave-height distribution measured during SUPERTANK ST_30A.

Figure 10. Cross-shore wave-height distribution measured during SUPERTANK ST_60A.

Figure 11. Cross-shore wave-height distribution measured during SUPERTANK ST_I0.

Figure 12. Cross-shore wave-height distribution for the LSTF spilling and plunging wave cases.

Figure 13. Wave runup measured during SUPERTANK ST_10A. The arrow with notation “ip” refers to the inflection point between the wave setup and runup.

Figure 14. Wave runup measured during SUPERTANK ST_30A. The arrow with notation “ip” refers to the inflection point between the wave setup and runup.

Figure 15. Wave runup measured during SUPERTANK ST_60A. The arrow with notation “ip” refers to the inflection point between the wave setup and runup.

780

781 Figure 16. Wave runup measured during SUPERTANK ST_I0. The arrow with notation
782 "ip" refers to the inflection point between the wave setup and runup.

783

784 Figure 17. Relationship between breaking wave height, upper limit of beach profile
785 change and wave runup for the thirty SUPERTANK cases examined.

786

787 Figure 18. Comparison of measured and predicted wave runup.

788

789 Figure 19. Forces acting on a water element in the swash zone.


SUPERTANK


LSTF

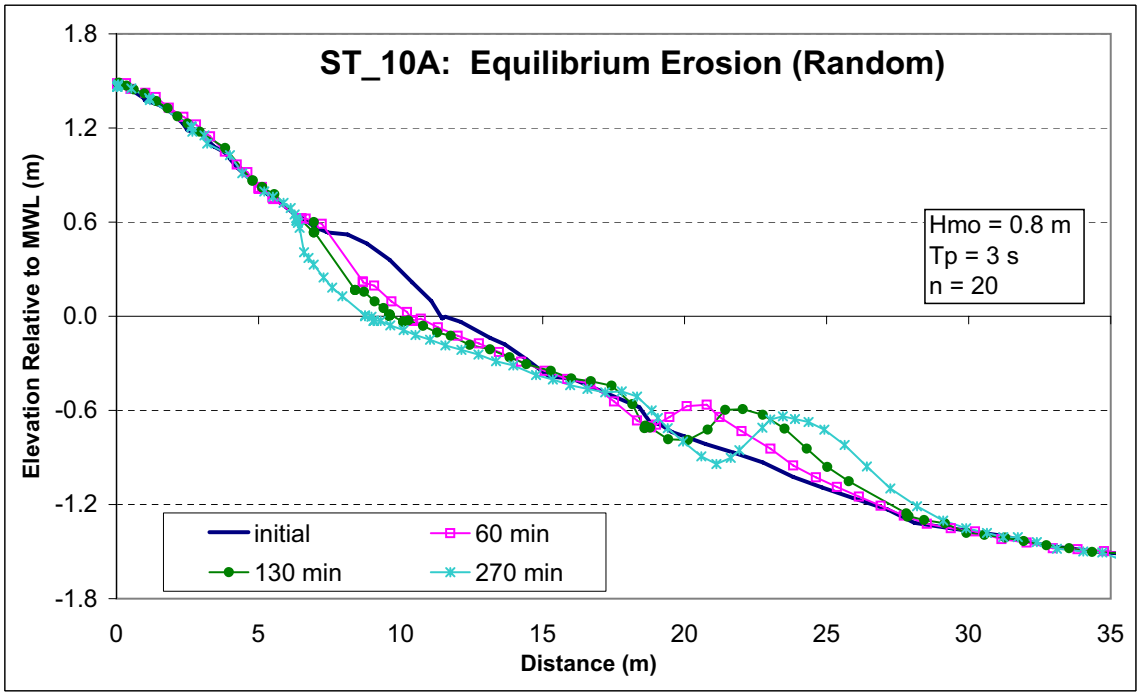
ST_10A: Equilibrium Erosion (Random)
Elevation Relative to MWL (m)
Distance (m)
1.8
1.2
0.6
0.0
-0.6
-1.2
-1.8
0
5
10
15
20
25
30
35
Hmo = 0.8 m
Tp = 3 s
n = 20
initial
60 min
130 min
270 min

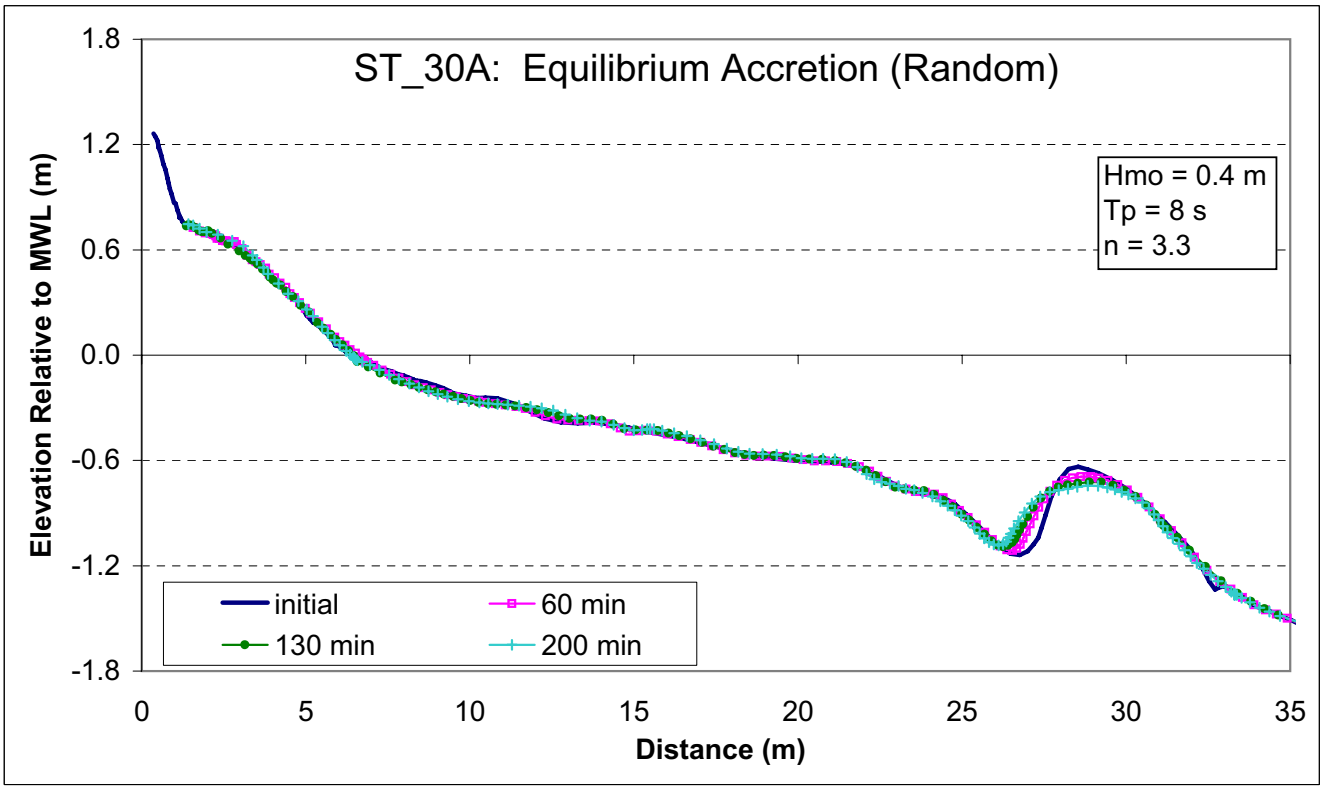
ST_30A: Equilibrium Accretion (Random)
Hmo = 0.4 m
Tp = 8 s
n = 3.3
initial
60 min
130 min
200 min
Elevation Relative to MWL (m)
Distance (m)
1.8
1.2
0.6
0.0
-0.6
-1.2
-1.8
0
5
10
15
20
25
30
35

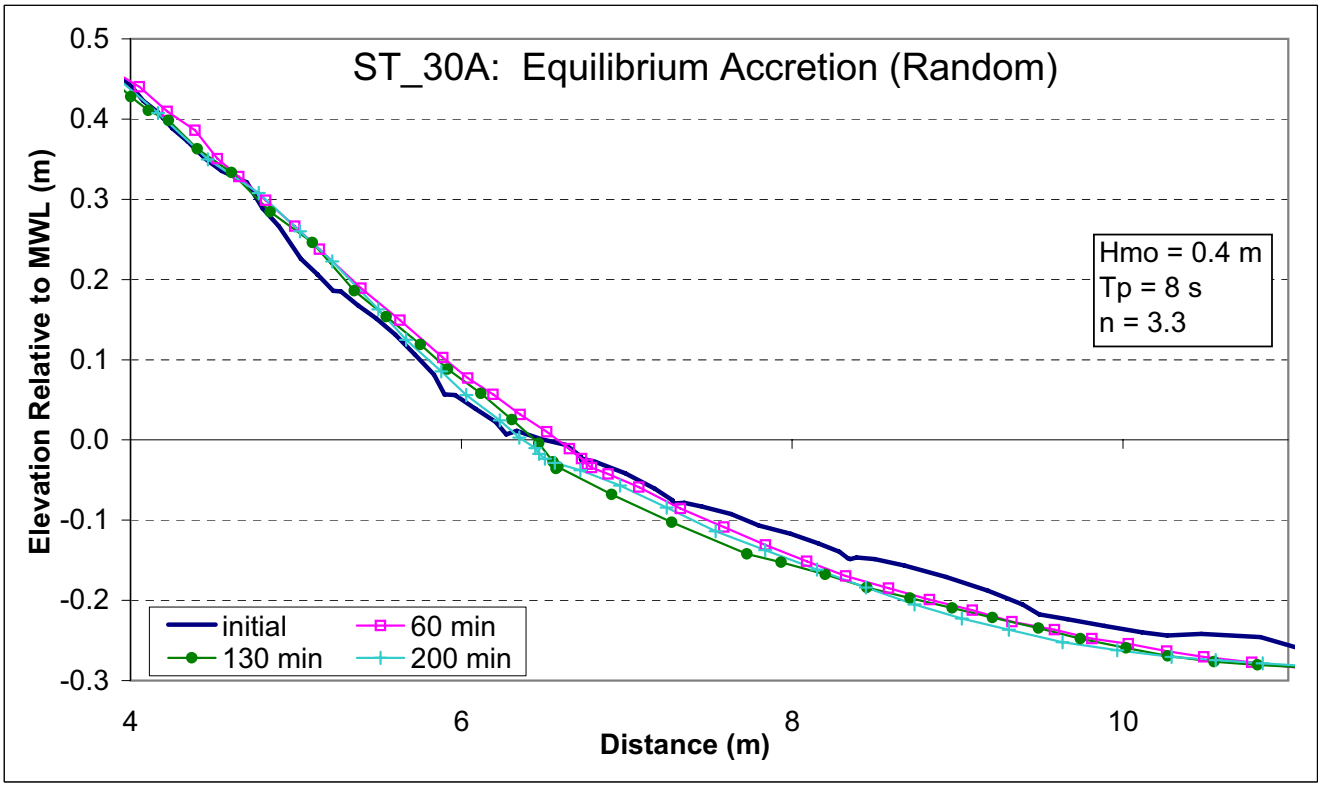
ST_30A: Equilibrium Accretion (Random)
Hmo = 0.4 m
Tp = 8 s
n = 3.3
initial
60 min
130 min
200 min
Elevation Relative to MWL (m)
Distance (m)
0.5
0.4
0.3
0.2
0.1
0.0
-0.1
-0.2
-0.3
4
6
8
10

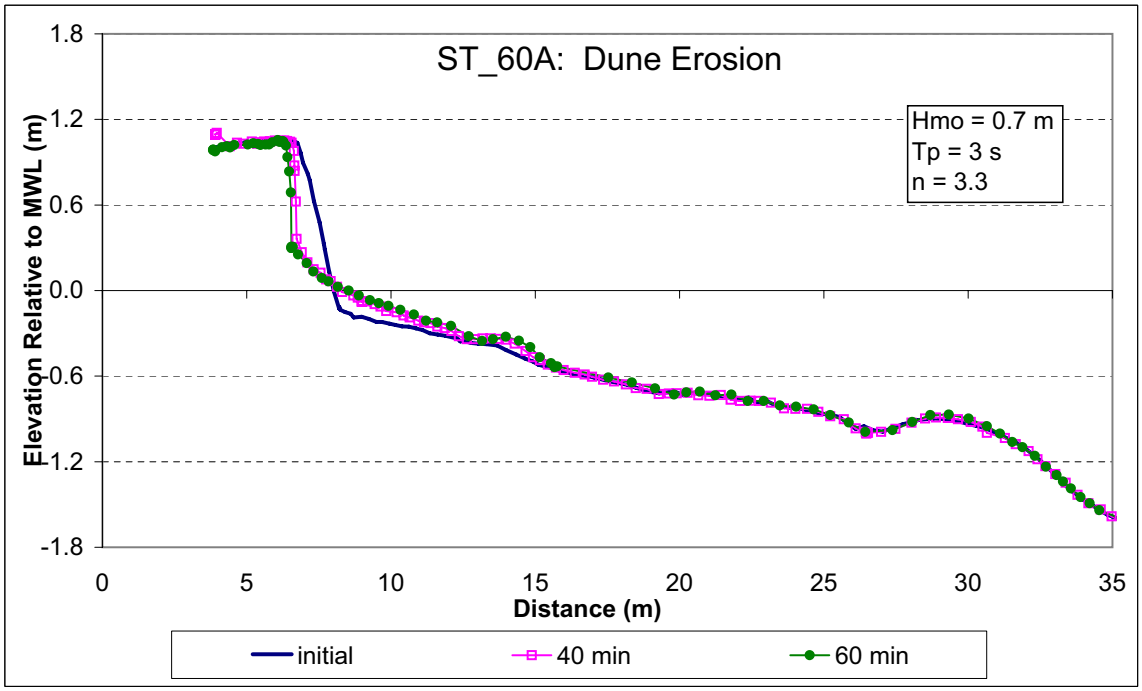
ST_60A: Dune Erosion
Hmo = 0.7 m
Tp = 3 s
n = 3.3
Elevation Relative to MWL (m)
1.8
1.2
0.6
0.0
-0.6
-1.2
-1.8
0
5
10
15
20
25
30
35
Distance (m)
initial
40 min
60 min

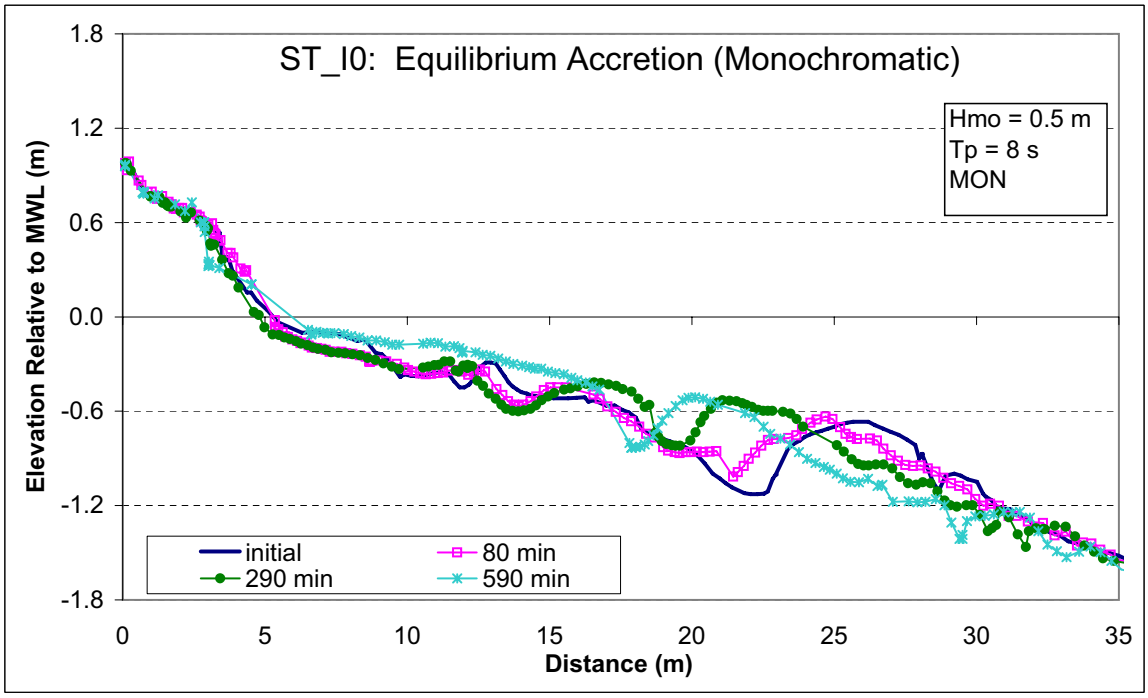
ST_I0: Equilibrium Accretion (Monochromatic)
Hmo = 0.5 m
Tp = 8 s
MON
Elevation Relative to MWL (m)
1.8
1.2
0.6
0.0
-0.6
-1.2
-1.8
0
5
10
15
20
25
30
35
Distance (m)
initial
80 min
290 min
590 min

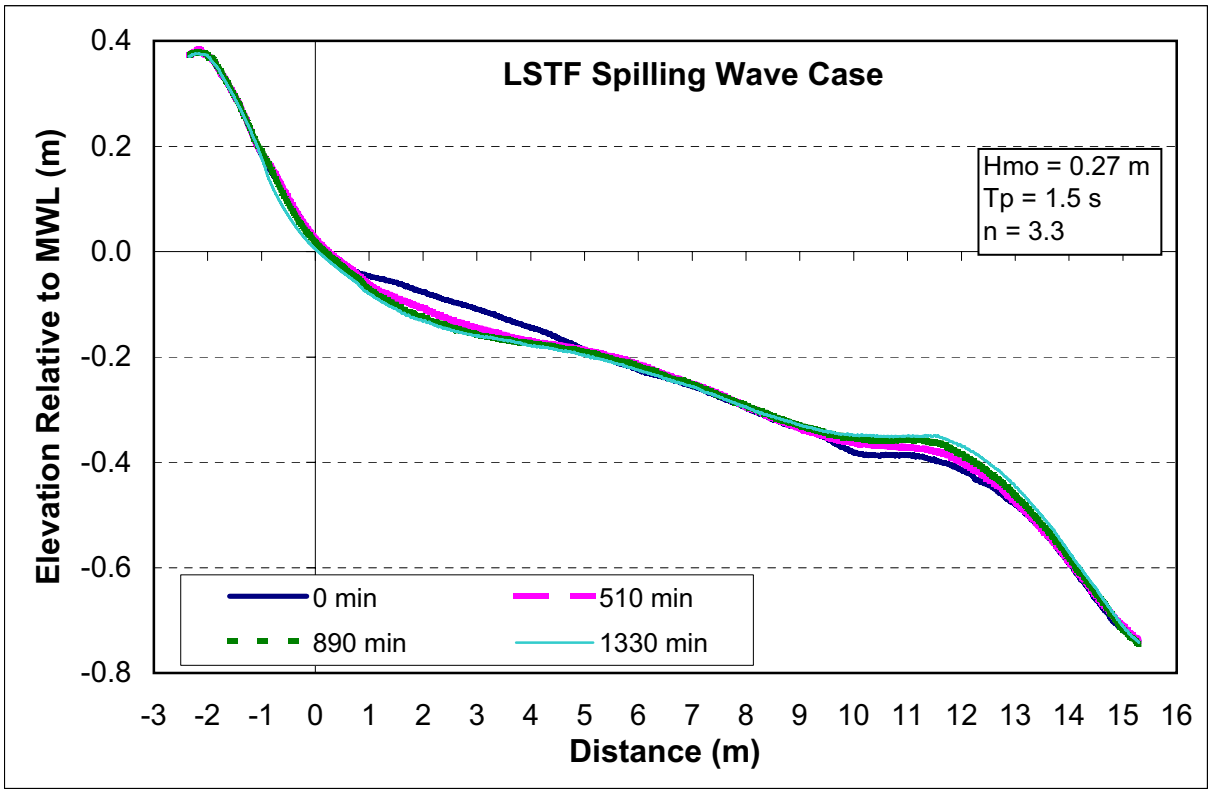
LSTF Spilling Wave Case
Hmo = 0.27 m
Tp = 1.5 s
n = 3.3
0 min
510 min
890 min
1330 min
Elevation Relative to MWL (m)
Distance (m)
0.4
0.2
0.0
-0.2
-0.4
-0.6
-0.8
-3 -2 -1 0 1 2 3 4 5 6 7 8 9 10 11 12 13 14 15 16

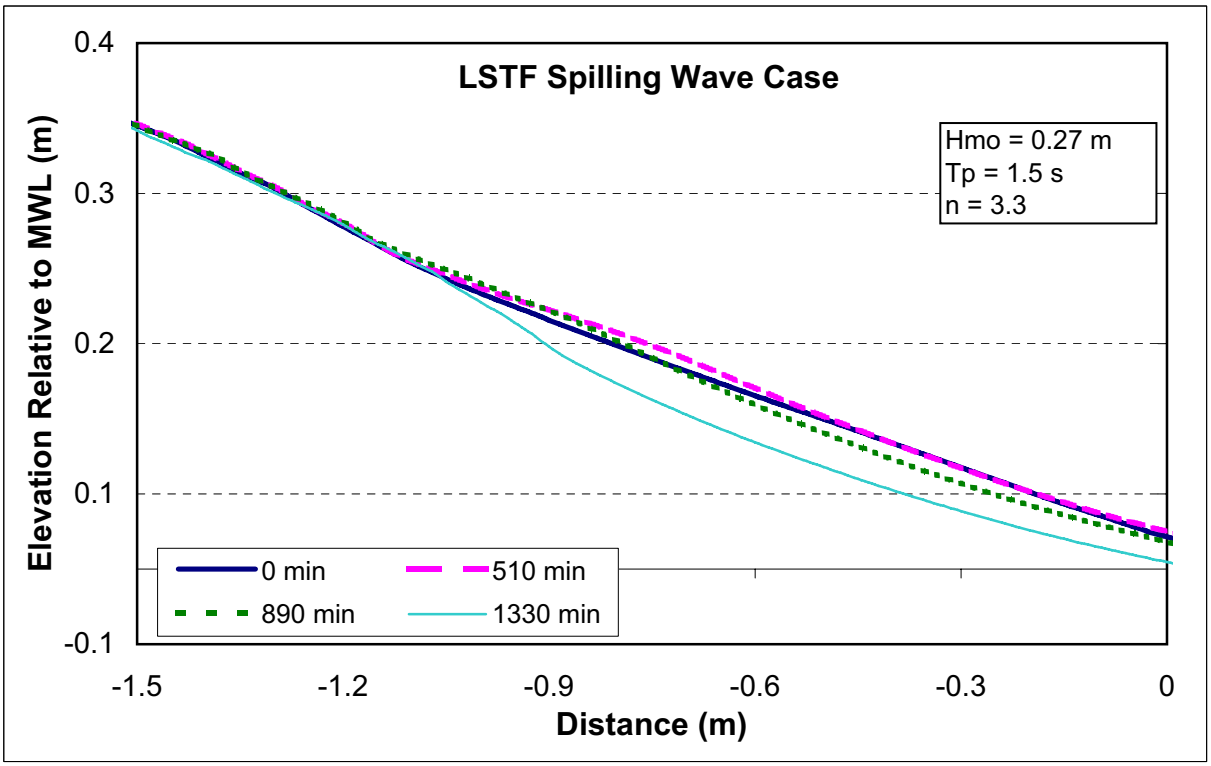
LSTF Spilling Wave Case
Hmo = 0.27 m
Tp = 1.5 s
n = 3.3
0 min
510 min
890 min
1330 min
Elevation Relative to MWL (m)
Distance (m)
0.4
0.3
0.2
0.1
-0.1
-1.5 -1.2 -0.9 -0.6 -0.3 0

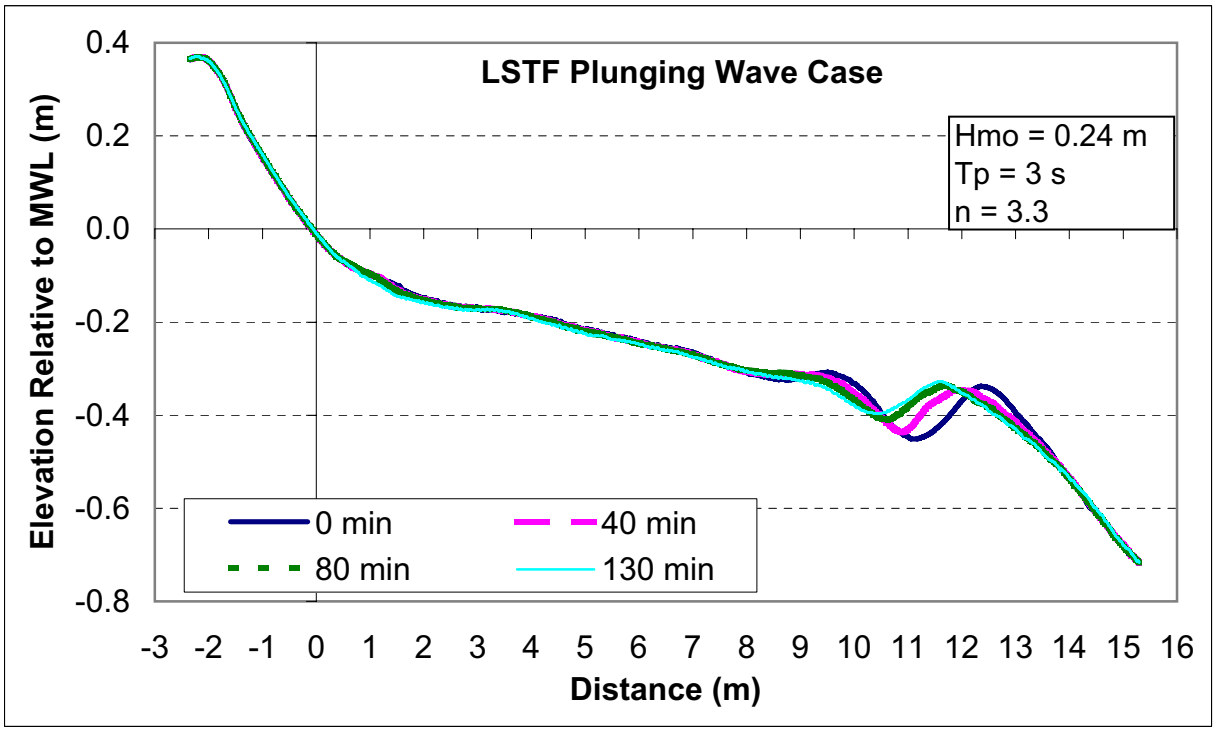
LSTF Plunging Wave Case
Hmo = 0.24 m
Tp = 3 s
n = 3.3
0 min
40 min
80 min
130 min
Elevation Relative to MWL (m)
Distance (m)
0.4
0.2
0.0
-0.2
-0.4
-0.6
-0.8
-3 -2 -1 0 1 2 3 4 5 6 7 8 9 10 11 12 13 14 15 16

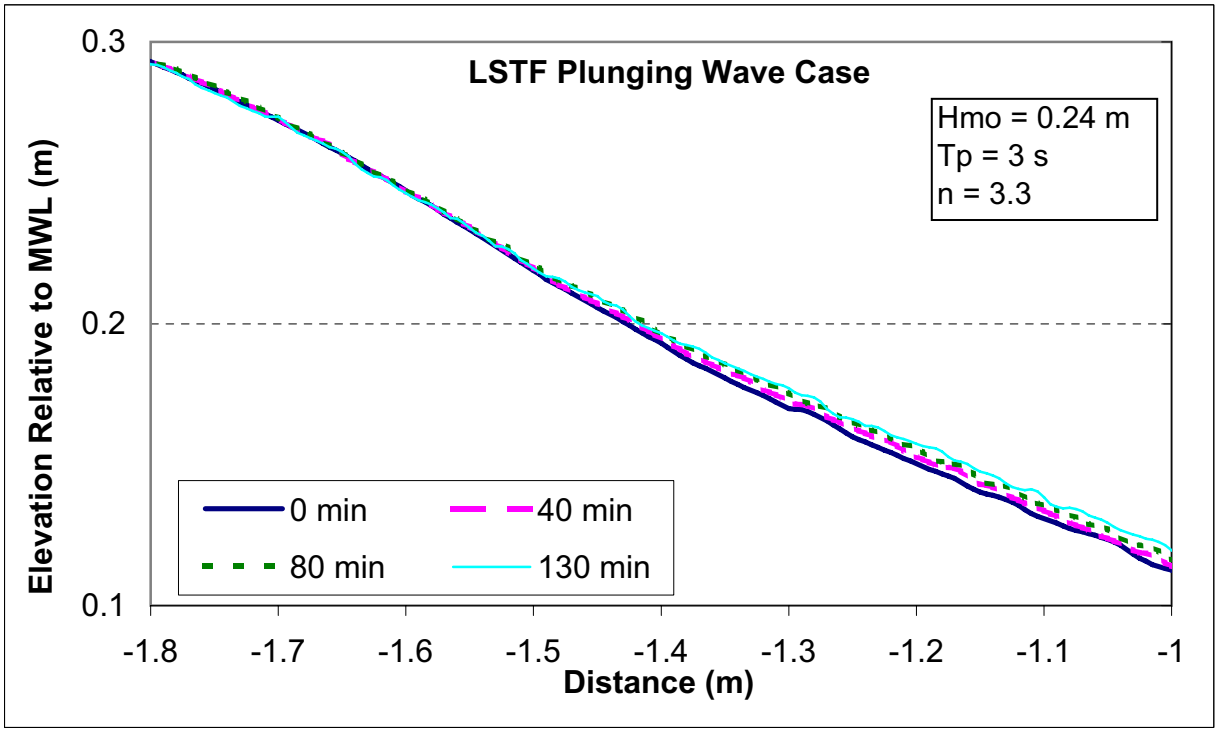
LSTF Plunging Wave Case
Hmo = 0.24 m
Tp = 3 s
n = 3.3
0 min
40 min
80 min
130 min
Elevation Relative to MWL (m)
Distance (m)
0.3
0.2
0.1
-1.8 -1.7 -1.6 -1.5 -1.4 -1.3 -1.2 -1.1 -1

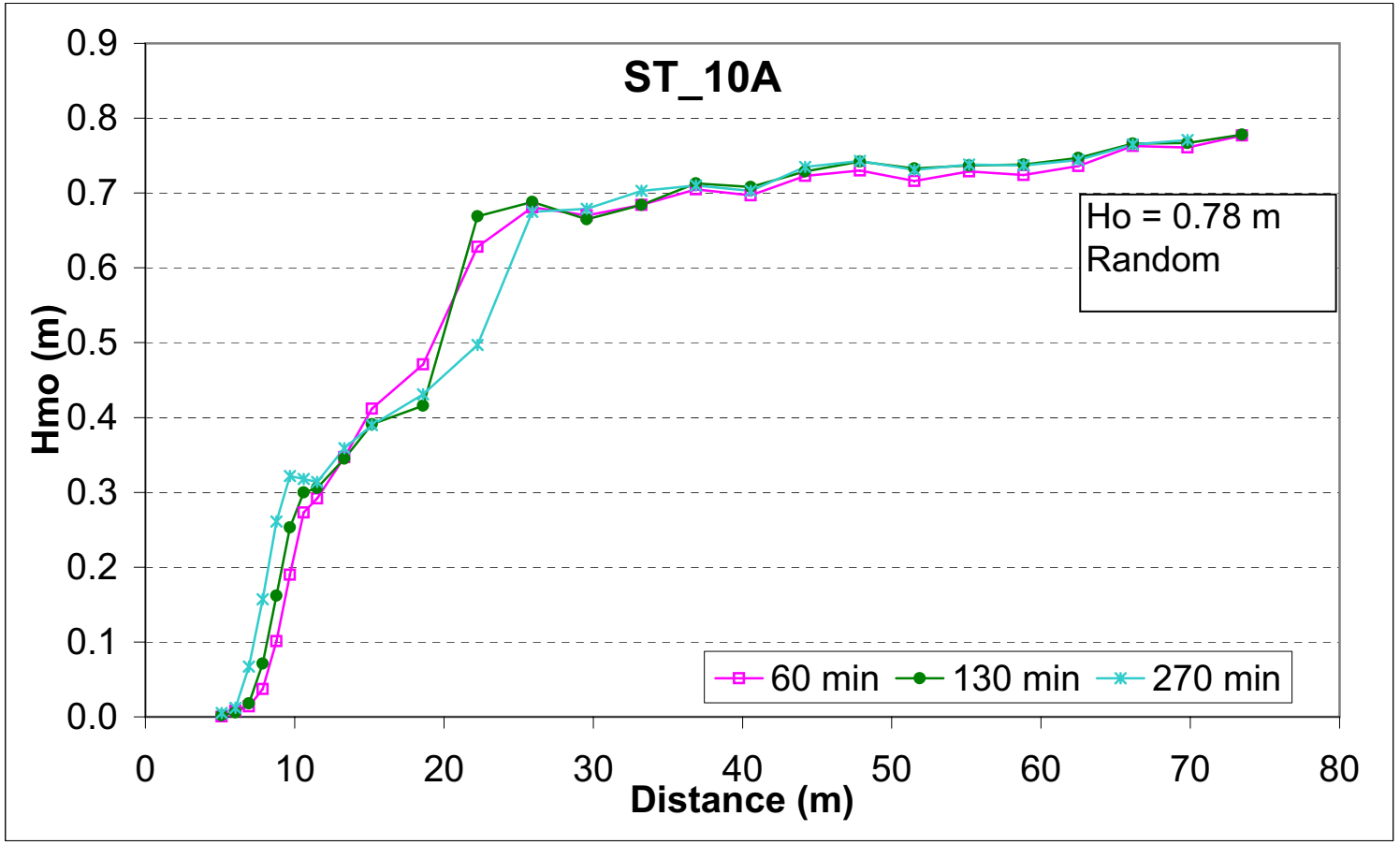
ST_10A
Ho = 0.78 m
Random
60 min
130 min
270 min
Hmo (m)
Distance (m)
0.0
0.1
0.2
0.3
0.4
0.5
0.6
0.7
0.8
0.9
0
10
20
30
40
50
60
70
80

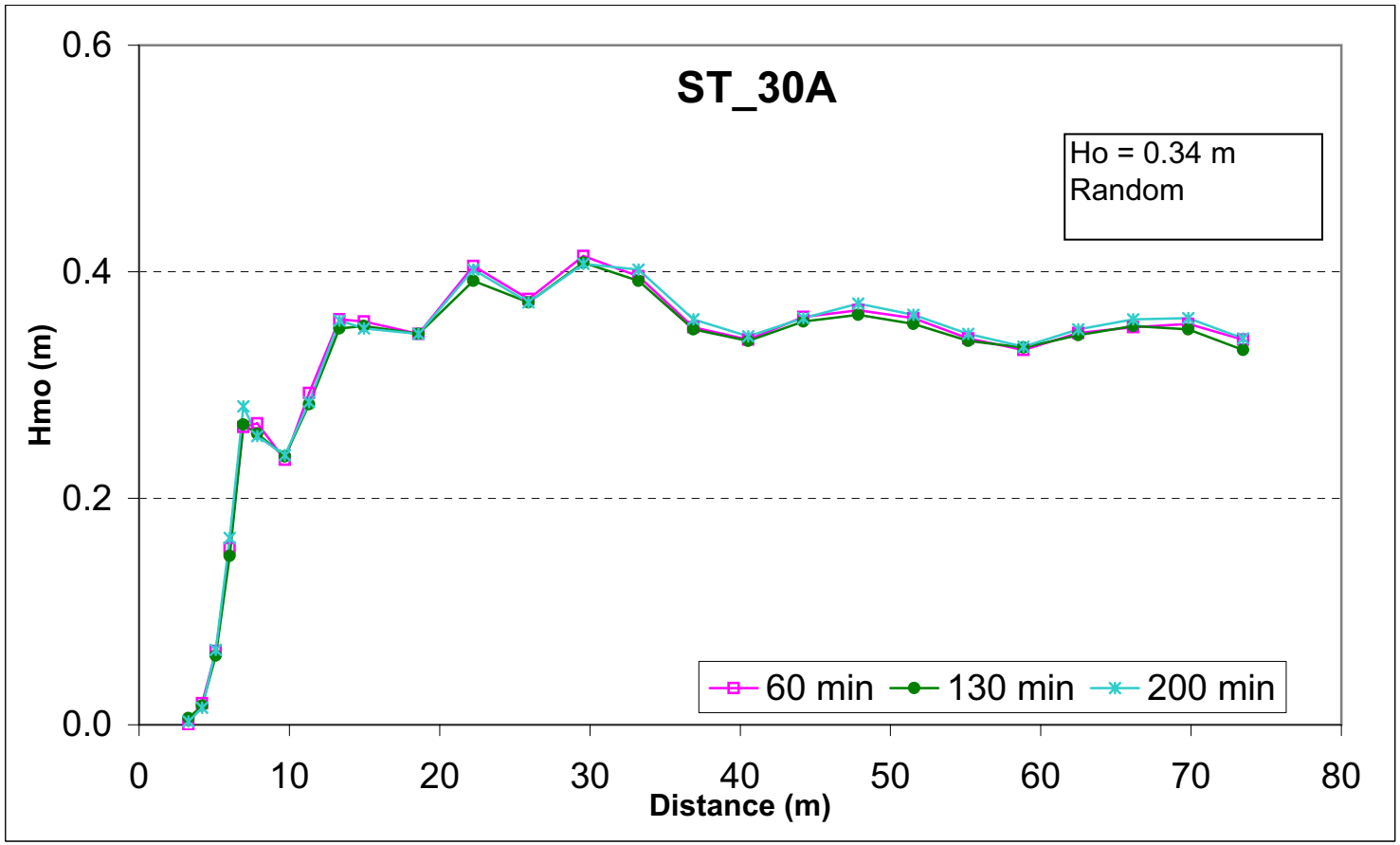
ST_30A
Ho = 0.34 m
Random
0.6
0.4
0.2
0.0
Hmo (m)
0
10
20
30
40
50
60
70
80
Distance (m)
60 min
130 min
200 min

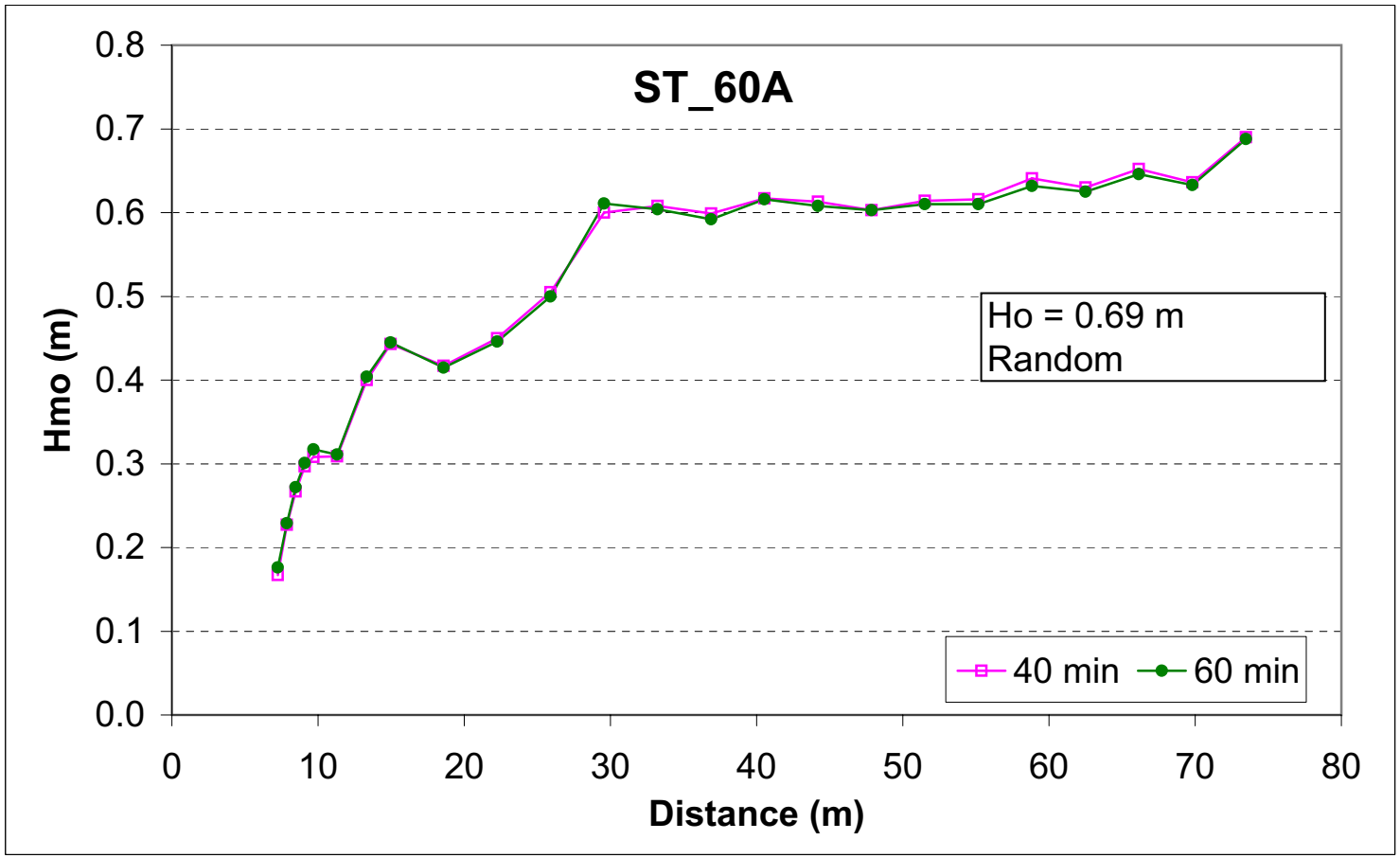
ST_60A
Hmo (m)
0.0
0.1
0.2
0.3
0.4
0.5
0.6
0.7
0.8
0
10
20
30
40
50
60
70
80
Distance (m)
Ho = 0.69 m
Random
40 min
60 min

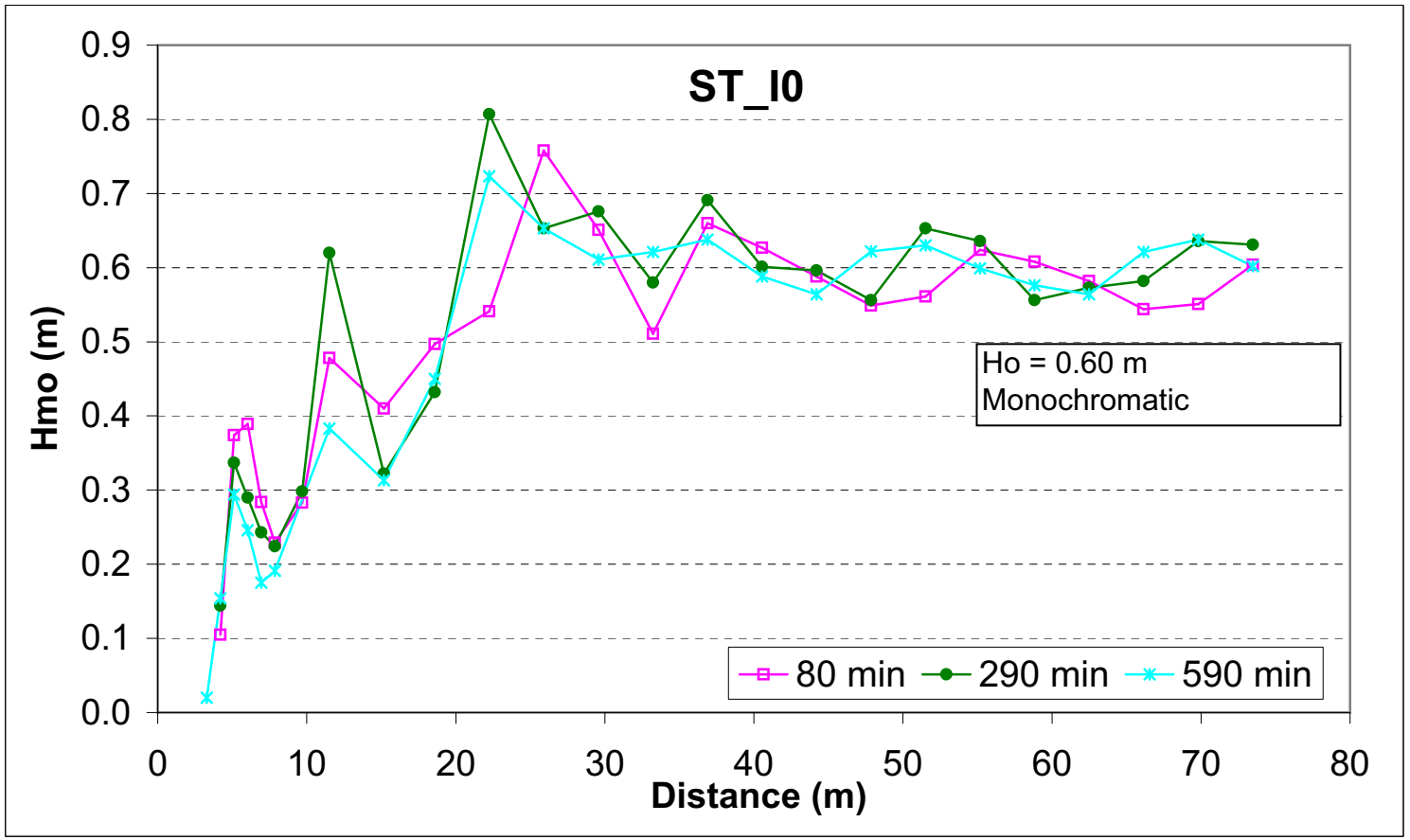
ST_I0
Hmo (m)
Distance (m)
0.0
0.1
0.2
0.3
0.4
0.5
0.6
0.7
0.8
0.9
0
10
20
30
40
50
60
70
80
Ho = 0.60 m
Monochromatic
80 min
290 min
590 min

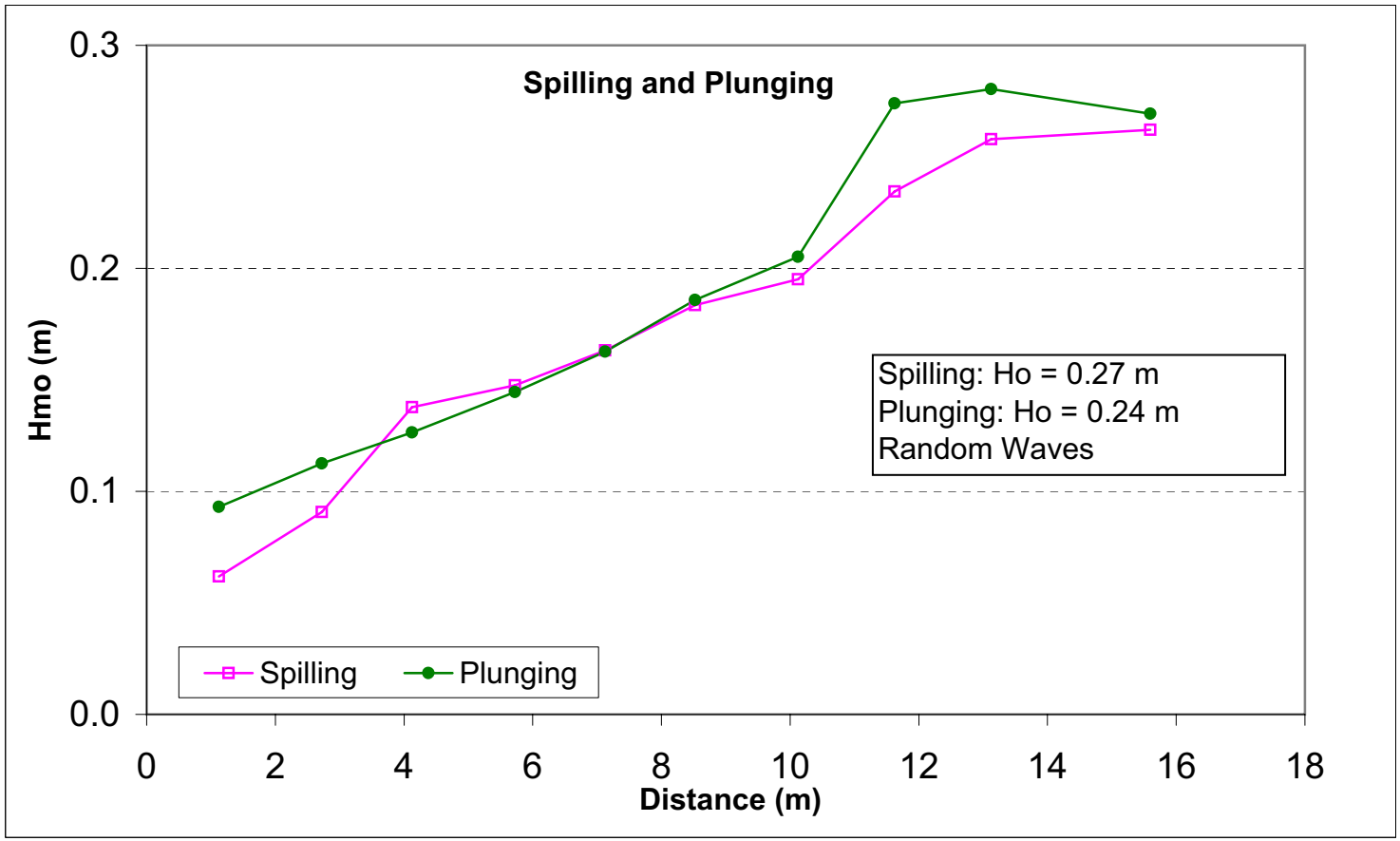
Spilling and Plunging
Hmo (m)
0.3
0.2
0.1
0.0
0
2
4
6
8
10
12
14
16
18
Distance (m)
Spilling: Ho = 0.27 m
Plunging: Ho = 0.24 m
Random Waves
Spilling
Plunging

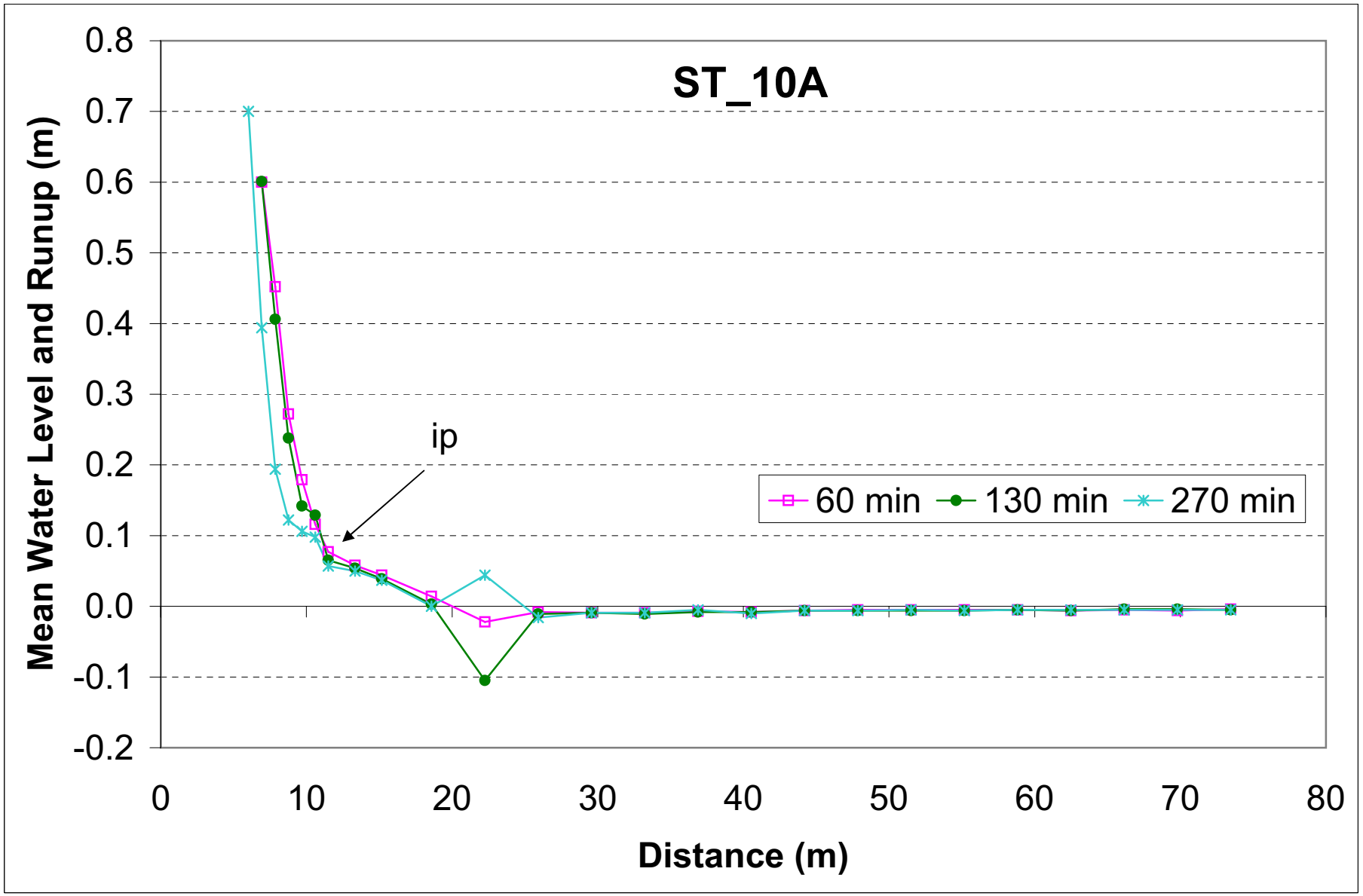
ST_10A
Mean Water Level and Runup (m)
0.8
0.7
0.6
0.5
0.4
0.3
0.2
0.1
0.0
-0.1
-0.2
ip
60 min
130 min
270 min
0
10
20
30
40
50
60
70
80
Distance (m)

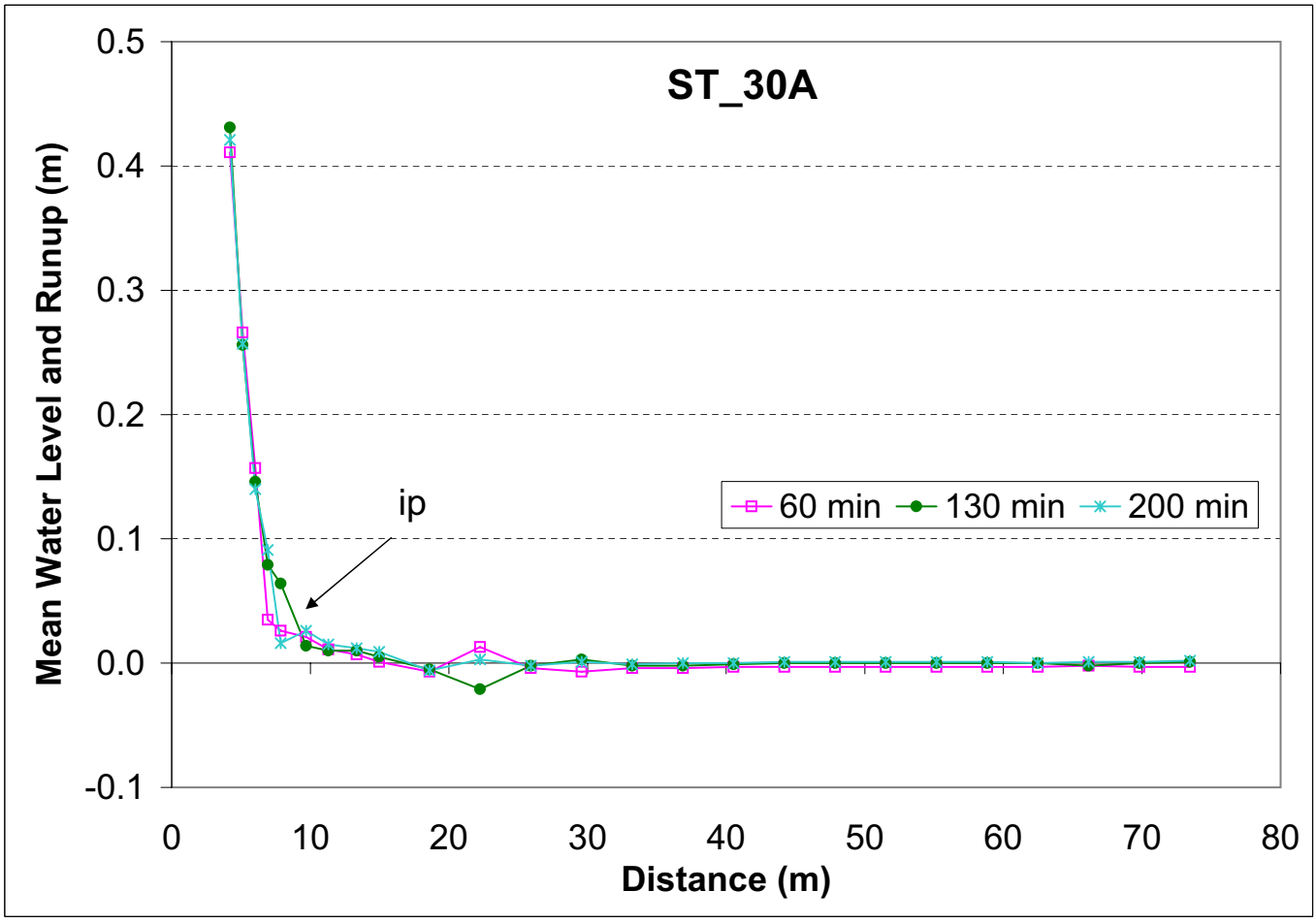
ST_30A
Mean Water Level and Runup (m)
0.5
0.4
0.3
0.2
0.1
0.0
-0.1
0
10
20
30
40
50
60
70
80
Distance (m)
ip
60 min
130 min
200 min

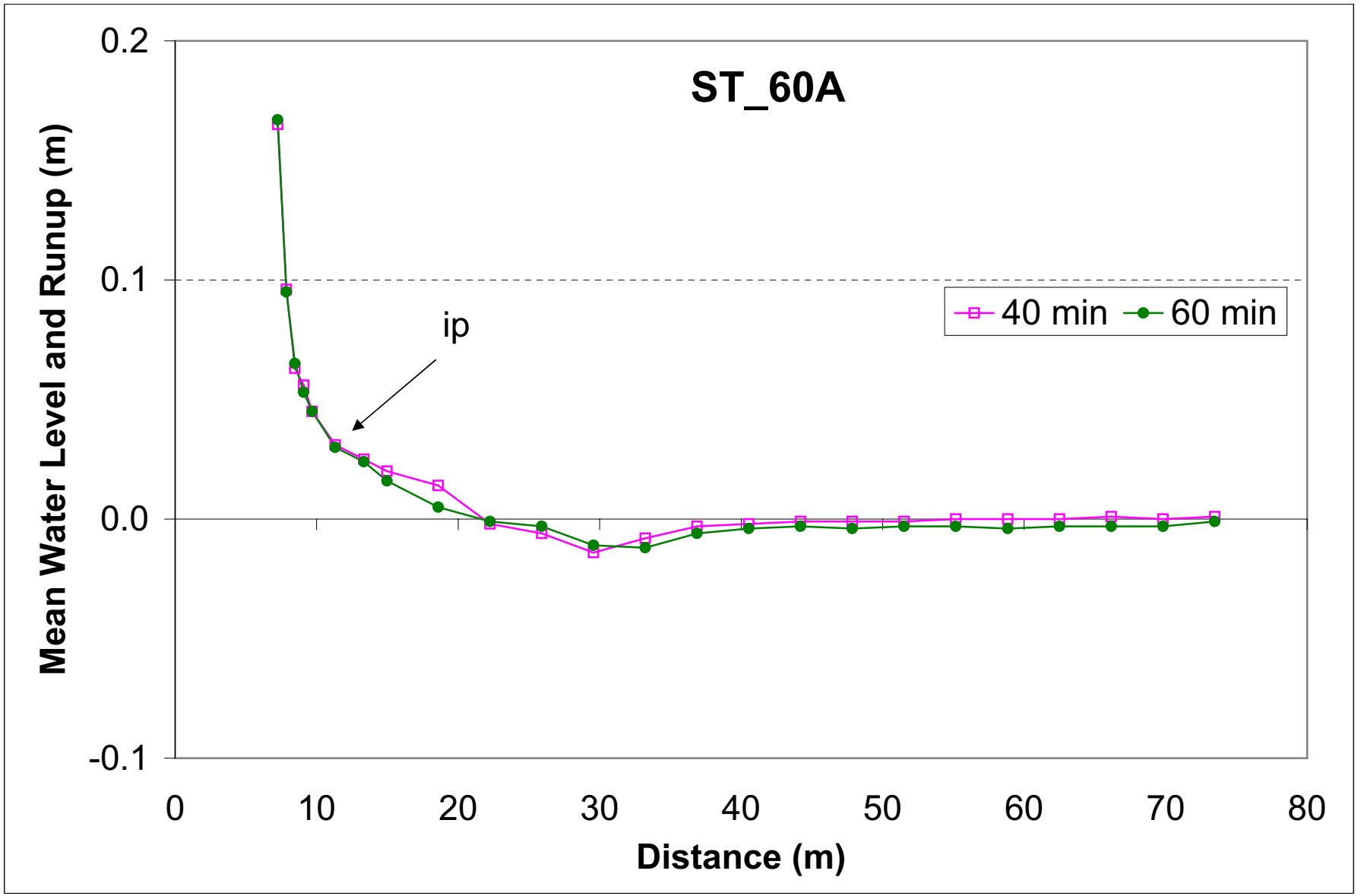
ST_60A
Mean Water Level and Runup (m)
0.2
0.1
0.0
-0.1
0
10
20
30
40
50
60
70
80
Distance (m)
ip
40 min
60 min

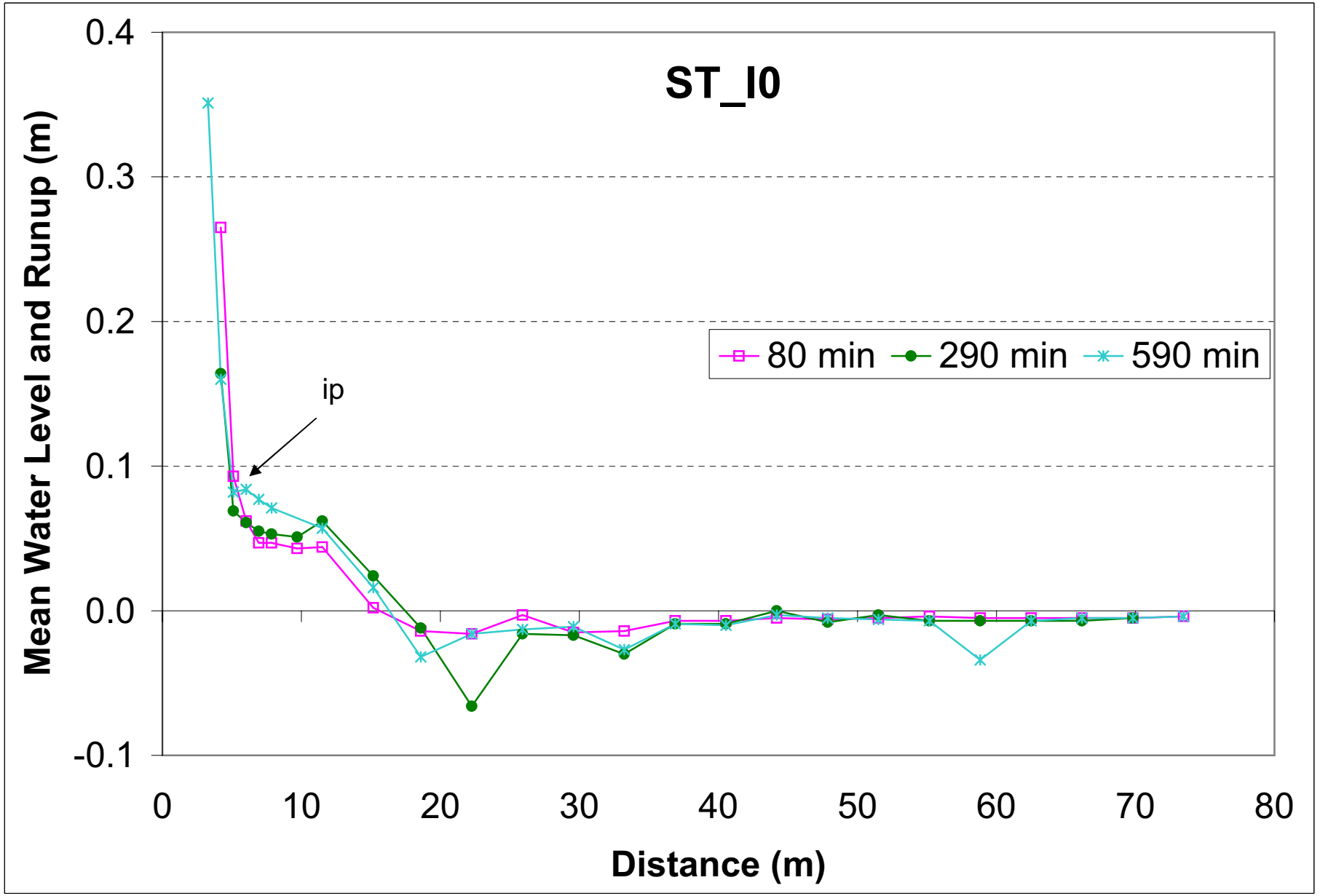
ST_I0
Mean Water Level and Runup (m)
0.4
0.3
0.2
0.1
0.0
-0.1
0
10
20
30
40
50
60
70
80
Distance (m)
80 min
290 min
590 min
ip

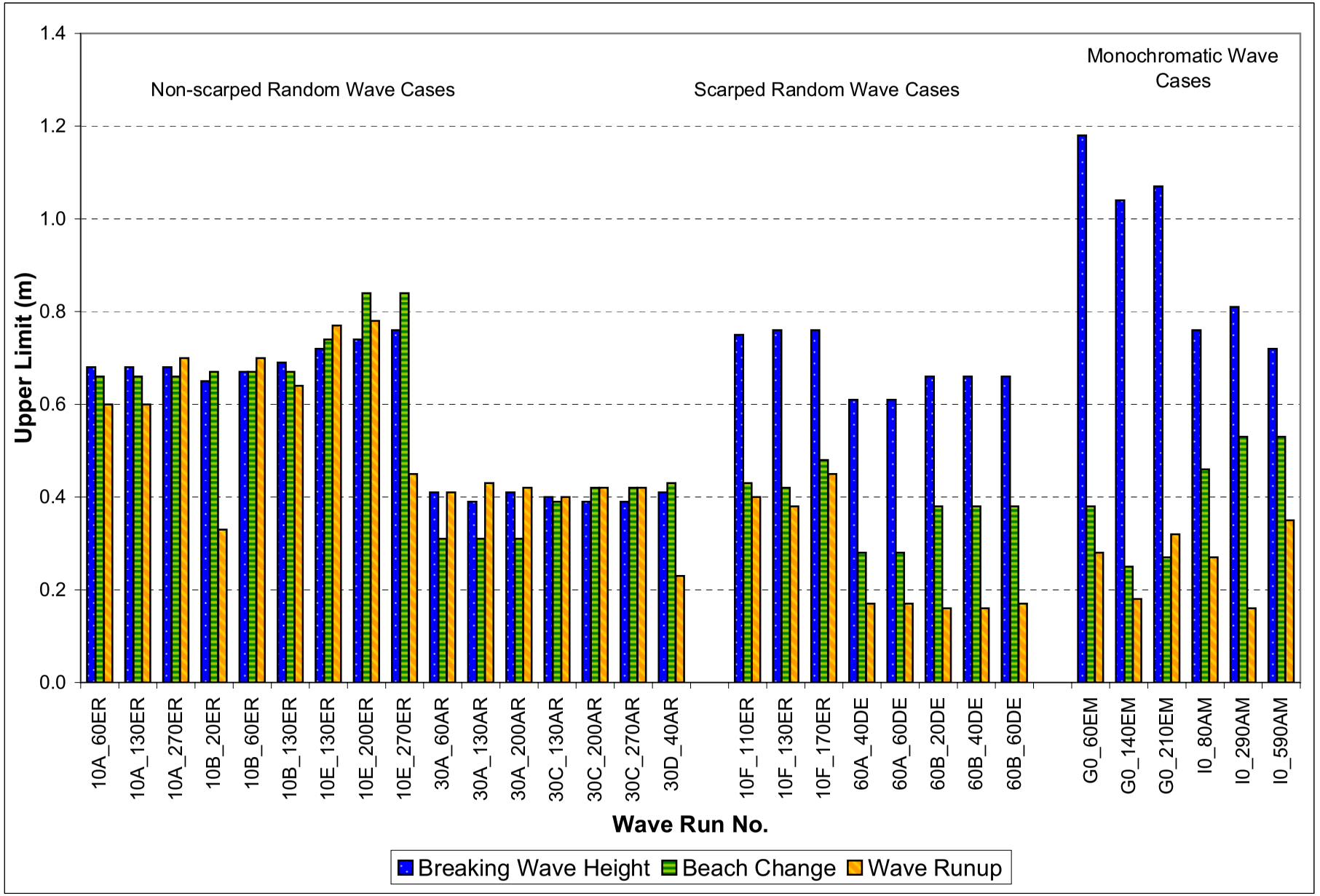
Non-scarped Random Wave Cases
Scarped Random Wave Cases
Monochromatic Wave Cases
Upper Limit (m)
1.4
1.2
1.0
0.8
0.6
0.4
0.2
0.0
10A_60ER
10A_130ER
10A_270ER
10B_20ER
10B_60ER
10B_130ER
10E_130ER
10E_200ER
10E_270ER
30A_60AR
30A_130AR
30A_200AR
30C_130AR
30C_200AR
30C_270AR
30D_40AR
10F_110ER
10F_130ER
10F_170ER
60A_40DE
60A_60DE
60B_20DE
60B_40DE
60B_60DE
G0_60EM
G0_140EM
G0_210EM
I0_80AM
I0_290AM
I0_590AM
Wave Run No.
Breaking Wave Height
Beach Change
Wave Runup

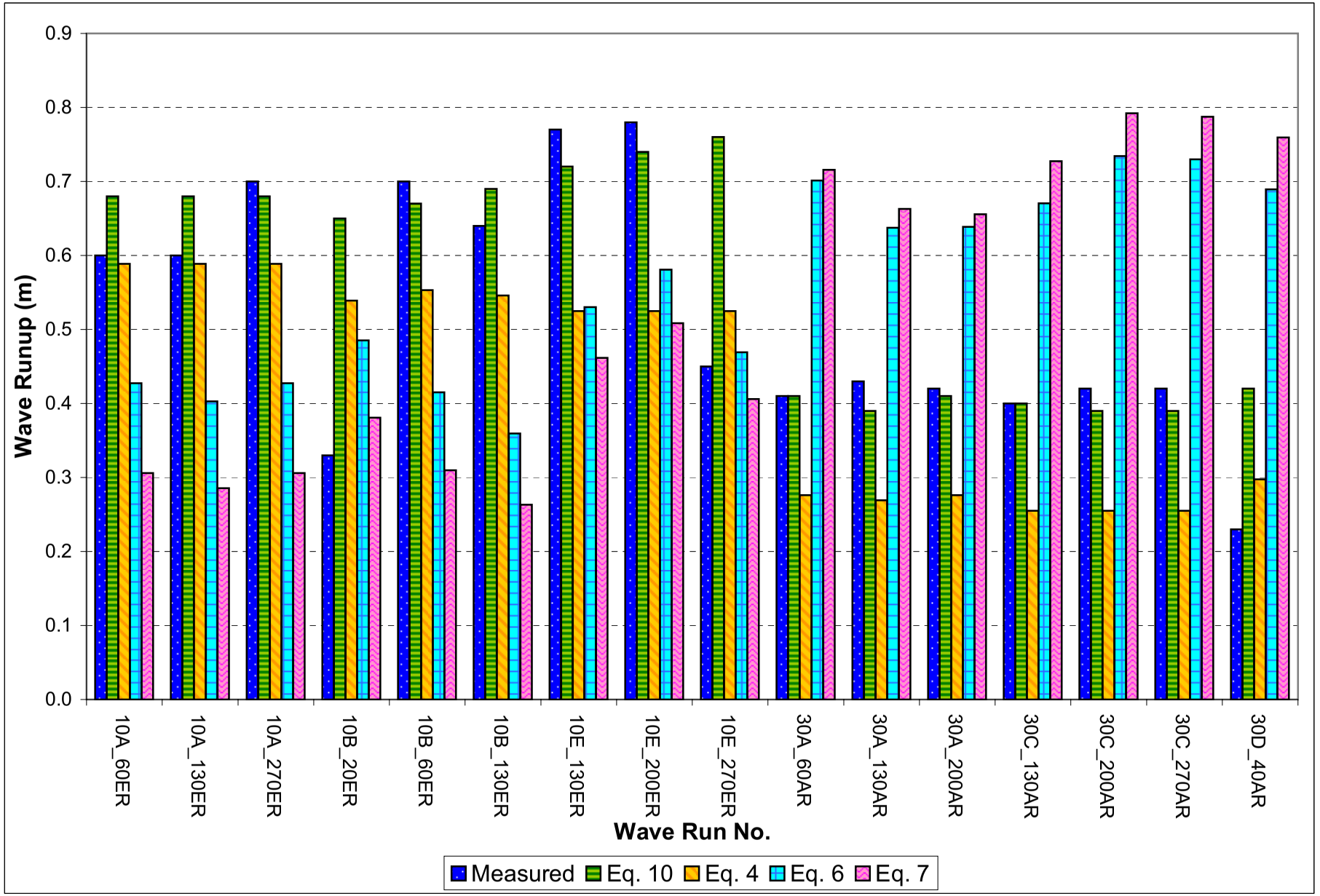
Wave Runup (m)
0.0
0.1
0.2
0.3
0.4
0.5
0.6
0.7
0.8
0.9
10A_60ER
10A_130ER
10A_270ER
10B_20ER
10B_60ER
10B_130ER
10E_130ER
10E_200ER
10E_270ER
30A_60AR
30A_130AR
30A_200AR
30C_130AR
30C_200AR
30C_270AR
30D_40AR
Wave Run No.
Measured
Eq. 10
Eq. 4
Eq. 6
Eq. 7

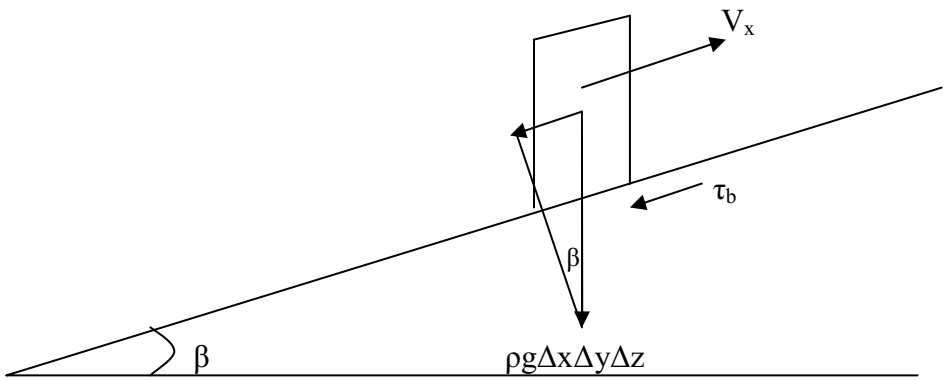
V_x
τ_b
β
β
ρgΔxΔyΔz

Table 1. Summary of Selected Wave Runs and Input Wave and Beach Conditions (Notation is explained at the bottom of the table).

Wave Run ID	H_o m	T_p s	L_o m	n	N	H_{bs} m	tanβ	ξ	H_{b_h} m	H_{b_l} m	H_{sl_h} m	H_{sl_l} m
SUPERTANK												
10A_60ER	0.78	3.0	14.0	20	6.4	0.68	0.10	0.42	0.66	0.15	0.13	0.24
10A_130ER	0.78	3.0	14.0	20	6.8	0.68	0.09	0.38	0.67	0.15	0.10	0.23
10A_270ER	0.78	3.0	14.0	20	6.9	0.68	0.10	0.42	0.65	0.16	0.10	0.24
10B_20ER	0.71	3.0	14.0	3.3	6.6	0.65	0.14	0.58	0.63	0.17	0.10	0.23
10B_60ER	0.73	3.0	14.0	3.3	6.8	0.67	0.11	0.44	0.65	0.17	0.11	0.24
10B_130ER	0.72	3.0	14.0	3.3	7.0	0.69	0.09	0.36	0.67	0.18	0.12	0.25
10E_130ER	0.69	4.5	31.6	20	4.9	0.72	0.11	0.69	0.71	0.15	0.15	0.16
10E_200ER	0.69	4.5	31.6	20	5.0	0.74	0.12	0.77	0.72	0.15	0.15	0.18
10E_270ER	0.69	4.5	31.6	20	5.1	0.76	0.09	0.58	0.74	0.15	0.16	0.20
10F_110ER	0.66	4.5	31.6	3.3	5.1	0.75	0.09	0.58	0.72	0.18	0.15	0.26
10F_130ER	0.68	4.5	31.6	3.3	5.1	0.76	0.08	0.48	0.74	0.18	0.13	0.21
10F_170ER	0.69	4.5	31.6	3.3	5.1	0.76	0.08	0.50	0.73	0.20	0.12	0.24
G0_60EM	1.05	3.0	14.0	M	10.0	1.18	0.10	0.43	1.18	0.01	0.11	0.03
G0_140EM	1.04	3.0	14.0	M	10.5	1.04	0.10	0.41	1.04	0.04	0.08	0.10
G0_210EM	1.15	3.0	14.0	M	10.8	1.07	0.09	0.39	1.07	0.04	0.11	0.02
30A_60AR	0.34	8.0	99.9	3.3	1.6	0.41	0.14	2.24	0.40	0.06	0.24	0.08
30A_130AR	0.33	8.0	99.9	3.3	1.6	0.39	0.13	2.09	0.38	0.06	0.24	0.09
30A_200AR	0.34	8.0	99.9	3.3	1.6	0.41	0.13	2.02	0.40	0.06	0.25	0.10
30C_130AR	0.31	9.0	126.4	20	1.4	0.40	0.13	2.36	0.40	0.04	0.18	0.05
30C_200AR	0.31	9.0	126.4	20	1.4	0.39	0.15	2.31	0.38	0.04	0.19	0.06
30C_270AR	0.31	9.0	126.4	20	1.4	0.39	0.15	2.60	0.38	0.04	0.20	0.06
30D_40AR	0.37	9.0	126.4	20	1.4	0.42	0.13	2.00	0.42	0.05	0.17	0.07
I0_80AM	0.60	8.0	99.9	M	2.9	0.76	0.20	2.78	0.76	0.01	0.38	0.03
I0_290AM	0.63	8.0	99.9	M	3.1	0.81	0.17	2.35	0.81	0.01	0.34	0.02
I0_590AM	0.60	8.0	99.9	M	2.7	0.72	0.12	1.64	0.73	0.01	0.25	0.03
60A_40DE	0.69	3.0	14.0	3.3	6.2	0.61	0.12	0.55	0.58	0.14	0.16	0.24
60A_60DE	0.69	3.0	14.0	3.3	6.2	0.61	0.10	0.46	0.60	0.14	0.12	0.24
60B_20DE	0.64	4.5	31.6	3.3	4.4	0.66	0.11	0.74	0.63	0.15	0.18	0.24
60B_40DE	0.63	4.5	31.6	3.3	4.4	0.66	0.11	0.76	0.62	0.16	0.18	0.25
60B_60DE	0.65	4.5	31.6	3.3	4.4	0.66	0.12	0.79	0.63	0.17	0.18	0.30
LSTF												
Spilling	0.27	1.5	3.5	3.3	10.0	0.26	0.11	0.41	N/C	N/C	N/C	N/C
Plunging	0.24	3.0	14.0	3.3	4.4	0.27	0.13	0.96	N/C	N/C	N/C	N/C

H_o = offshore wave height; T_p = peak wave period; L_o = offshore wavelength; n = spectral peakedness; N = Dean Number; H_{bs} = significant breaking wave height; tan β = beach slope defined as the slope of the section approximately 1 m landward and 1 m seaward of the shoreline; ξ = surf similarity parameter; H_{b_h} = incident band wave height at the breaker line; H_{b_l} = low frequency band wave height at the breaker line; H_{sl_h} = incident band wave height at the shoreline; H_{sl_l} = low-frequency band wave height at the shoreline; M = monochromatic wave; N/C = Not calculated.

Table 2. Summary of Beach Change and Breaking Wave Height

Wave Run ID	H_{bs} m	U_L m	L_L m	Scarp
SUPERTANK				
10A_60ER	0.68	0.66	1.29	No
10A_130ER	0.68	0.66	1.29	No
10A_270ER	0.68	0.66	1.29	No
10B_20ER	0.65	0.67	1.35	No
10B_60ER	0.67	0.67	1.35	No
10B_130ER	0.69	0.67	1.35	No
10E_130ER	0.72	0.74	1.52	No
10E_200ER	0.74	0.84	1.52	No
10E_270ER	0.76	0.84	1.52	No
10F_110ER	0.75	0.43	1.52	Yes
10F_130ER	0.76	0.42	1.52	Yes
10F_170ER	0.76	0.48	1.52	Yes
G0_60EM	1.18	0.38	1.61	No
G0_140EM	1.04	0.25	1.61	Yes
G0_210EM	1.07	0.27	1.61	Yes
30A_60AR	0.41	0.31	1.36	No
30A_130AR	0.39	0.31	1.36	No
30A_200AR	0.41	0.31	1.36	No
30C_130AR	0.40	0.39	1.01	No
30C_200AR	0.39	0.42	1.01	No
30C_270AR	0.39	0.42	1.01	No
30D_40AR	0.42	0.43	0.65	No
I0_80AM	0.76	0.46	1.82	No
I0_290AM	0.81	0.53	1.82	No
I0_590AM	0.72	0.53	1.82	Yes
60A_40DE	0.61	0.28	1.16	Yes
60A_60DE	0.61	0.28	1.16	Yes
60B_20DE	0.66	0.38	0.99	Yes
60B_40DE	0.66	0.38	0.99	Yes
60B_60DE	0.66	0.38	0.99	Yes
LSTF				
Spilling	0.26	0.23	0.62	No
Plunging	0.27	0.26	0.50	No

U_L, L_L = upper and lower limit of beach change, respectively.

Table 3. Summary of Measured and Predicted Wave Runup.

Wave Run ID	H_{bs} m	R_{tw} m	Eq 4 m	Eq 6 m	Eq 7 m	Eq 10 m
10A_60ER	0.68	0.60	**0.59**	0.43	0.31	**0.68**
10A_130ER	0.68	0.60	**0.59**	0.40	0.29	**0.68**
10A_270ER	0.68	0.70	0.59	0.43	0.31	**0.68**
10B_20ER	0.65	0.33	0.54	0.49	**0.38**	0.65
10B_60ER	0.67	0.70	0.55	0.42	0.31	**0.67**
10B_130ER	0.69	0.64	**0.55**	0.36	0.26	**0.69**
10E_130ER	0.72	0.77	0.52	0.53	0.46	**0.72**
10E_200ER	0.74	0.78	0.52	0.58	0.51	**0.74**
10E_270ER	0.76	0.45	**0.52**	**0.47**	**0.41**	0.76
30A_60AR	0.41	0.41	0.28	0.70	0.72	**0.41**
30A_130AR	0.39	0.43	0.27	0.64	0.66	**0.39**
30A_200AR	0.41	**0.42**	**0.28**	0.64	0.66	**0.41**
30C_130AR	0.40	0.40	0.25	0.67	0.73	**0.40**
30C_200AR	0.39	0.42	0.25	0.73	0.79	**0.39**
30C_270AR	0.39	0.42	0.25	0.73	0.79	**0.39**
30D_40AR	0.42	0.23	0.30	0.69	0.76	0.42

Bold font indicates predicted values that fall within 15% of the measured runup. R_{tw} = total measured wave runup.